

Connecting substellar and stellar formation. The role of the host star's metallicity.

J. Maldonado¹, E. Villaver², C. Eiroa², and G. Micela¹

¹ INAF - Osservatorio Astronomico di Palermo, Piazza del Parlamento 1, 90134 Palermo, Italy
e-mail: jesus.maldonado@inaf.it

² Universidad Autónoma de Madrid, Dpto. Física Teórica, Facultad de Ciencias, Campus de Cantoblanco, 28049 Madrid, Spain

Received September 15, 1996; accepted March 16, 1997

ABSTRACT

Context. Most of our current understanding of the planet formation mechanism is based on the planet metallicity correlation derived mostly from solar-type stars harbouring gas-giant planets.

Aims. To achieve a far more reaching grasp on the substellar formation process we aim to analyse in terms of their metallicity a diverse sample of stars (in terms of mass and spectral type) covering the whole range of possible outcomes of the planet formation process (from planetesimals to brown dwarfs and low-mass binaries).

Methods. Our methodology is based on the use of high-precision stellar parameters derived by our own group in previous works from high-resolution spectra by using the iron ionisation and equilibrium conditions. All values are derived in an homogeneous way, except for the M dwarfs where a methodology based on the use of pseudo equivalent widths of spectral features was used.

Results. Our results show that as the mass of the substellar companion increases the metallicity of the host star tendency is to lower values. The same trend is maintained when analysing stars with low-mass stellar companions and a tendency towards a wide range of host star's metallicity is found for systems with low mass planets. We also confirm that more massive planets tend to orbit around more massive stars.

Conclusions. The core-accretion formation mechanism for planet formation achieves its maximum efficiency for planets with masses in the range 0.2 and 2 M_{Jup} . Substellar objects with higher masses have higher probabilities of being formed as stars. Low-mass planets and planetesimals might be formed by core-accretion even around low-metallicity stars.

Key words. techniques: spectroscopic - stars: abundances -stars: late-type -stars: planetary systems

1. Introduction

Exoplanetary science has succeeded in discovering an astonishing diversity of planetary systems. The role of the host star's metallicity in planet formation has been largely discussed with the finding that the frequency of giant planets is a strong function of the stellar metallicity (Gonzalez 1997; Santos et al. 2004; Fischer & Valenti 2005). The planet-metallicity correlation is usually interpreted in the framework of the core-accretion model (e.g. Pollack et al. 1996) as the final mass of cores via oligarchic growth increases with the solid density in proto-planetary discs (Kokubo & Ida 2002).

Initially found for gas-giant planets around solar-type stars (Gonzalez 1997; Fischer & Valenti 2005), many works have tried to probe whether the gas-giant planet metallicity correlation also holds for other kind of stars as well as other types of substellar objects, e.g. low-mass planets (Ghezzi et al. 2010b; Mayor et al. 2011; Sousa et al. 2011; Buchhave et al. 2012; Buchhave & Latham 2015), brown dwarfs (Sahlmann et al. 2011; Ma & Ge 2014; Mata Sánchez et al. 2014; Maldonado & Villaver 2017), stars with debris discs (Beichman et al. 2005; Chavero et al. 2006; Greaves et al. 2006; Bryden et al. 2009; Kóspál et al. 2009; Maldonado et al. 2012, 2015b; Gáspár et al. 2016), evolved (sub-giant and red giant) stars (Sadakane et al. 2005; Schuler et al. 2005; Hekker & Meléndez 2007; Pasquini et al. 2007; Takeda et al. 2008; Ghezzi et al. 2010a; Maldonado et al. 2013; Mortier et al. 2013; Jofré et al. 2015; Reffert et al. 2015; Maldonado

& Villaver 2016), low-mass (M dwarf) stars (e.g. Neves et al. 2013), or if there are differences in the host star metallicity when close-in and more distant planets are present in the system (Sozzetti 2004; Maldonado et al. 2018; Wilson et al. 2018). It should be noted that most of these references refer to radial velocity planets.

As clear from the references above, previous works focus on particular types of stars and planets and, to the very best of our knowledge, a global view of the planet-metallicity correlation and its implications on the planet formation process are still missing. This is precisely the goal of this work in which we analyse in the most homogeneous possible way a large sample of stars harbouring the full range of possible outcomes of the planet formation process (from debris discs to massive brown dwarfs) and without any restriction of the host star's spectral type (from M dwarfs to early-F) or evolutionary status (from main-sequence to giants). The analysis is completed with literature data of low-mass binary stars in order to set the results into a general context.

The paper is organised as follows. Section 2 describes the stellar sample. The completeness of the planet host subsample is analysed in Sect. 3. The analysis of the host star metallicities as a function of the substellar companion mass and the mass of the host star is performed in Sect. 4. The results are discussed in the context of current planet formation models in Sect. 5. A comparison with the results from the KEPLER mission is performed in Sect. 6. Our conclusions follow in Sect. 7.

Table 1. Architecture of the planetary systems in our stellar sample.

Type	Number	Notes
Substellar objects (total)	345	95 multiple systems
Brown dwarfs ($10 M_{\text{Jup}} < m_{\text{C}} \sin i < 70 M_{\text{Jup}}$)	59	3 systems with 2 BDs 5 systems BD + planet
Low-mass planets ($m_{\text{C}} \sin i < 30 M_{\oplus}$)	78	34 hot ($a < 0.1$ au) 44 cool ($a > 0.1$ au)
Gas-giant planets ($m_{\text{C}} \sin i > 30 M_{\oplus}$)	208	34 hot ($a < 0.1$ au) 174 cool ($a > 0.1$ au)
Debris disc	99	32 Debris disc + substellar object

2. Stellar sample

Our stellar sample is selected from our previous works (Maldonado et al. 2012, 2013, 2015a,b, 2018; Maldonado & Villaver 2016, 2017) which might be consulted for further details. Briefly, high-resolution échelle spectra of the stars were obtained in 2-3 metre class telescopes or obtained from public archives. Basic stellar parameters (T_{eff} , $\log g$, microturbulent velocity ξ_t , and $[\text{Fe}/\text{H}]$) were determined by using the code TGVIT¹ (Takeda et al. 2005) which implements the iron ionisation, match of the curve of growth and iron equilibrium conditions. Stellar age, mass, and radius were computed from HIPPARCOS V magnitudes (ESA 1997) and parallaxes (van Leeuwen 2007), when available, using the code PARAM² (da Silva et al. 2006), together with the PARSEC set of isochrones (Bressan et al. 2012). For some planet hosts where the PARAM code failed to give a reasonable value we took the mass values from the NASA exoplanet archive (specifically from the summary of stellar information table, for all stars but KOI 415 for which we took the value from the KOI stellar properities table). For the M dwarfs a different methodology was used. The analysis is based on the use of ratios of pseudo equivalent widths of spectral features which are sensitive to the effective temperature and the stellar metallicity (Maldonado et al. 2015a). Stellar masses and luminosities for M dwarfs were obtained from the derived temperatures and metallicities by using empirical calibrations.

The total number of stars in our sample amounts to 551. It is composed of 71 F-type stars, 261 G-type stars, 166 K-type stars, and 53 early-Ms. Regarding their evolutionary state, 373 are in the main-sequence, 63 are classified as subgiants, and 115 are giants.

The different architectures of the planetary systems harboured by our sample (type and number of substellar objects) are shown in Table 1, while figure 1 shows the Hertzsprung-Russell (HR) diagram of the stars analysed. Our sample is mainly composed of “mature” planetary systems as only $\sim 7\%$ of our stars have estimated ages younger than 500 Myr.

3. Sample completeness

A deep analysis of the completeness or detectability of our planet host sample is difficult to overcome as our targets are not selected from any particular exoplanet survey. Indeed, they were initially selected to address different individual aspects of the planet formation process (presence of discs, planet formation around evolved stars, brown-dwarf vs. planet formation, hot vs. cool planets ...). Our planet host sample includes targets from different radial velocity surveys, e.g., the HARPS search for southern extra-solar planets (Pepe et al. 2004); the Anglo-Australian planet search (Tinney et al. 2001); the N2K survey (Fischer

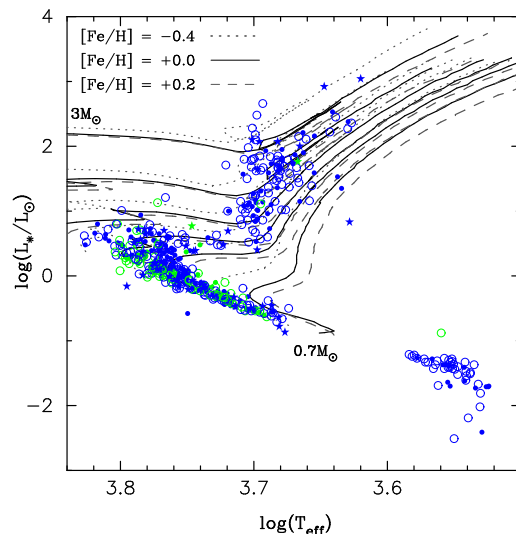


Fig. 1. Luminosity versus T_{eff} diagram for the stars analysed. Stars with discs are plotted as green whilst stars without discs are shown in blue. Stars with planets are shown as filled circles and stars with companions in the brown dwarf regime are shown in filled stars. Some evolutionary tracks ranging from 0.7 to 3.0 solar masses from Girardi et al. (2000) are overplotted. For each mass, three tracks are plotted, corresponding to $Z = 0.008$ ($[\text{Fe}/\text{H}] = -0.4$ dex, dotted lines), $Z = 0.019$ ($[\text{Fe}/\text{H}] = +0.0$ dex, solid lines), and $Z = 0.030$ ($[\text{Fe}/\text{H}] = +0.20$ dex, dashed lines).

et al. 2005); the UCO/Lick survey (Hekker et al. 2006); the the PennState-Torun Centre for Astronomy Planet Search (Niedzielski & Wolszczan 2008); the retired A stars project (Johnson et al. 2007); or the list of stars with brown dwarf companions by Ma & Ge (2014) and Wilson et al. (2016); among others. In other words, our planet host sample comes from a wide variety of planet search programmes with (most likely) different selection criteria, sensibilities, and biases, sampling significantly different regions of the HR diagram.

On the other hand, the comparison sample is mainly drawn from the HIPPARCOS catalogue (ESA 1997) and was chosen to cover similar stellar parameters as the stars with detected planets. For the sake of completeness, we give in Table A.1 the basic properties of the full sample of stars covered here. Further details can be found in our previous works (see references above).

In order to estimate the detectability limits of our planet hosts we proceeded as follows. For each star we searched for its corresponding radial velocity curve. Whenever possible, radial velocity data was taken from the NASA Exoplanet Archive³. Otherwise, we searched for the data in the corresponding discovery’s paper. We were able to recover the radial velocity series for 89.6% of our stars with planets. We subtracted the contribution of the known planets to each radial velocity data set by fitting a keplerian orbit using the code *rvlin*⁴ (Wright & Howard 2009). The fits were done by fixing the planetary period to the published values. When several planets were present around the same star, we subtract them in a sequential way. We took into account the fact that data obtained with different instruments might be available for the same star. Once the contribution for the known planets have been removed from the radial velocity

¹ <http://optik2.mtk.nao.ac.jp/~takeda/tgv/>

² <http://stev.oapd.inaf.it/cgi-bin/param>

³ <https://exoplanetarchive.ipac.caltech.edu>

⁴ <http://exoplanets.org/code/>

datasets, we considered the rms of the residuals to be representative of our measurement uncertainty (e.g. Endl et al. 2001).

For each planet host we computed the expected radial velocity semiamplitude due to the presence of different types of planets considering circular orbits, as usually done in the literature (see e.g. Mayor et al. 2011, and references therein). We also note that it has been shown that even eccentricities as high as 0.5 do not have a strong influence in the planet detection’s limits (Endl et al. 2002; Cumming & Dragomir 2010). We sampled the planetary mass space in logarithmic space, with values ranging from 0.005 to 80 M_{Jup} . Regarding the orbital periods, we sampled the orbital frequencies (also in logarithmic space) from periods from one to 10^4 days. For each planet we computed the expected radial velocities keeping the same time as the original observations. A total of eleven realizations of the radial velocity, each simulation corresponding to a different phase offset (from 0 to 2π), were performed. We considered a planet to be detectable around a given star if the rms of the planet’s expected radial velocity is larger than the rms of the stellar radial velocity residuals in each of the simulated phases (Galland et al. 2005; Lagrange et al. 2012; Meunier et al. 2012). We are aware that this is a “conservative” approach, i.e., it might overestimate the detection limits for some periods. It is however, a fast and robust method, ideal for achieving a quick look an for obtaining an efficient determination of the detection limits (Meunier et al. 2012). It should be noted that for the scope of this work a conservative approach should be preferred in order to obtain robust conclusions.

Figure 2 shows the derived detection probability curves. They show for each period, the percentage of stars from our sample for which planets with the corresponding minimum mass might be detected, i.e., planets located in the region above the $p\%$ curve can be detected in $p\%$ of our stars.

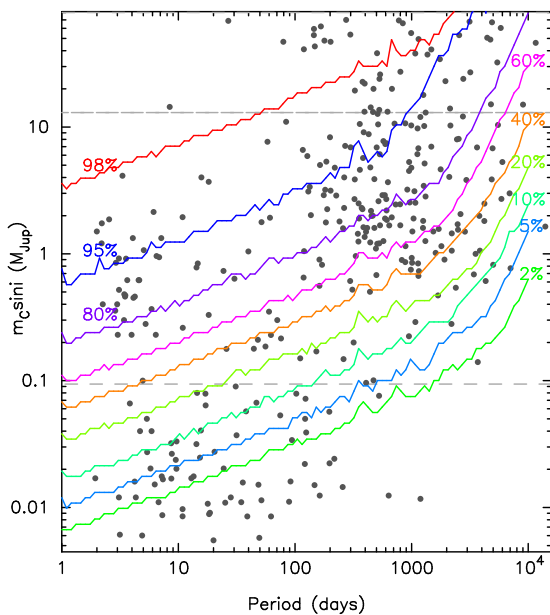


Fig. 2. Minimum mass versus planetary period diagram. Substellar companions analysed in this work are shown in grey circles. Detection probability curves are superimposed with different colours. Horizontal dashed lines indicate the standard mass loci of low-mass planets, and gas-giant planets companions.

Several main conclusions can be drawn from this plot: i) First, most of the long-period planets ($P > 100$ days) are detectable in approximately more than 60-80% of our targets. Only for planets with periods longer than ~ 2000 days with a mass of the order of few Jupiter masses and lower, our detectability fraction decreases to $\sim 40\%$ and below; ii) Low-mass planets, on the other hand, are detectable only in a small fraction of stars, between 2 and 20%; iii) Finally, it can be seen that planets with the mass of Jupiter and short periods are detectable in practically all stars.

As noted before our approach is quite conservative, so it is not surprising that some planets are actually located in the region under the 2% probability curve. We will discuss at length the implications of these findings in our analysis in the next sections.

Figure 3 shows the detectability limits for different subsamples of interest, see Sect. 4. In addition to the conclusions from the previous figure it can be seen the detectability curves for surveys aiming to detect low-mass planets are clearly shifted towards lower planetary mass companions, as expected. On the other hand surveys of stars with brown dwarfs and specially surveys of giant stars show significant higher detection limits. Stars with cool and hot Jupiters show nearly identical detection curves. Finally, we can see that we are mostly insensitive to the presence of small planets (specially evident in the case of surveys around evolved stars) which demonstrates the need of dedicated intensive long-term surveys (and probably the development of specific techniques to deal with the stellar noise problem) in order to detect this kind of planets.

4. Analysis

Figure 4 compares the cumulative distribution function of the stellar metallicity of the different stars analysed in this work. The stars have been divided into stars hosting hot Jupiters (if planets are located at distances smaller than 0.1 au), stars hosting cool distant-gas-giant planets, giant stars with planets, stars harbouring low-mass brown dwarfs ($m_C \sin i < 42.5 M_{\text{Jup}}$), stars with high-mass brown dwarfs ($m_C \sin i > 42.5 M_{\text{Jup}}$), stars harbouring only low-mass planets ($m_C \sin i < 30 M_{\oplus}$), and stars hosting only debris discs. The figure shows that while the metallicity distribution of stars with hot and cool gas-giant planets are shifted towards high metallicity values, this is not the case for the other samples, which show metallicity distributions consistent with that of the comparison sample (i.e., stars without substellar companions).

Figure 5 shows the host star metallicity as a function of the (minimum) mass of the substellar companion. Colours and symbols indicate the mass of the host star. The figure clearly shows a tendency of lower host star’s metallicities as the mass of the substellar companion increases. The figure also shows that more massive planets tend to orbit around more massive stars. It is clear from the figure that there is lack of planets around stars with metallicities lower than ~ -0.4 dex. Stars with metallicities below this limit only harbour substellar companions in the brown dwarf regime. We note that this result reeferes to our sample and several planetary companions around more metal poor stars have been found.

Our results suggest that there is a non universal planet formation mechanism. Different mechanisms may operate altogether and their relative efficiency change with the mass of the substellar object that is formed. For substellar objects with masses in the range $30 M_{\oplus} - 1 M_{\text{Jup}}$, high host star metallicities are found, suggesting that these planets are mainly formed by the core-accretion mechanism. As we move towards more massive sub-

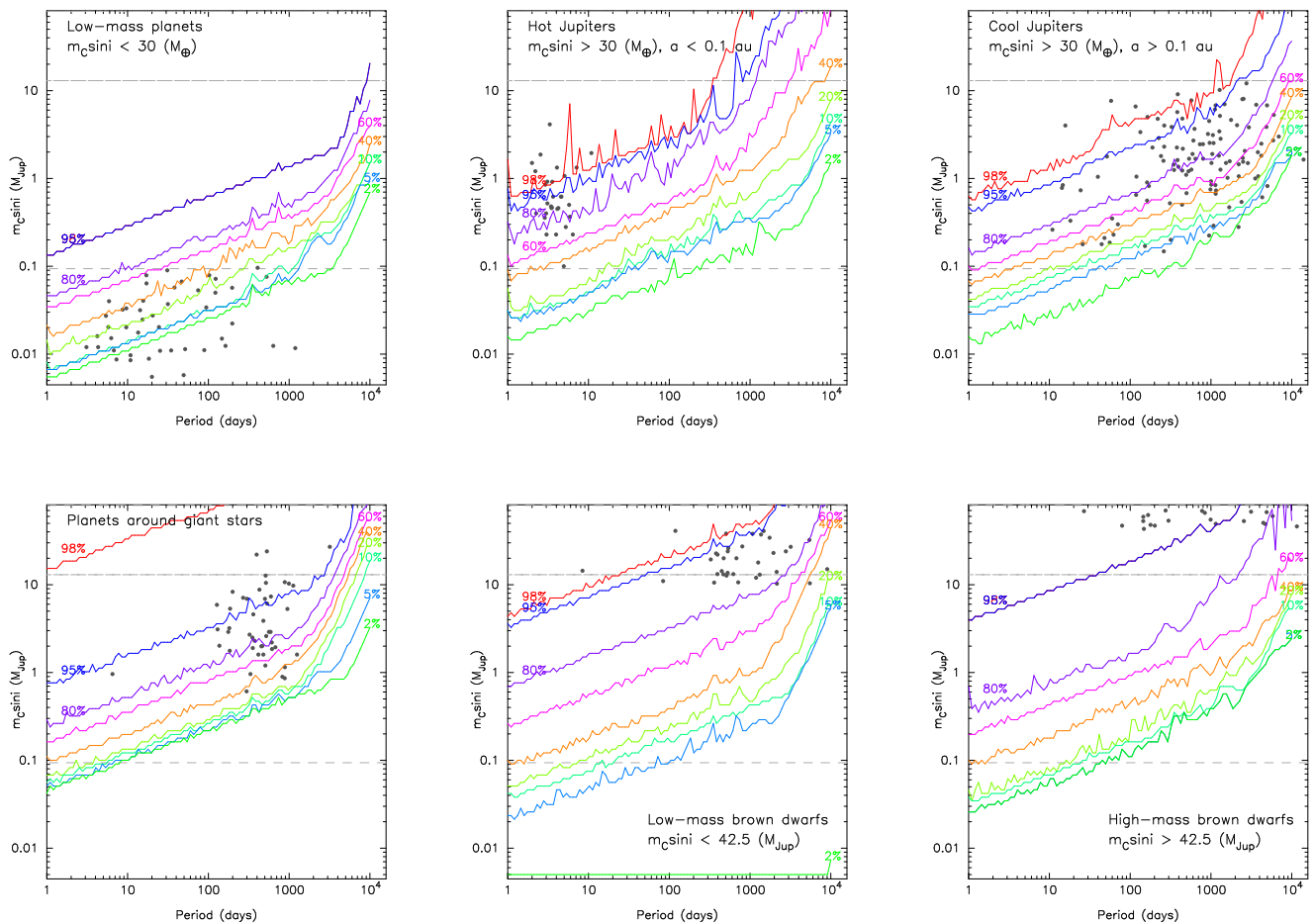


Fig. 3. Same as Fig. 2 but for the different subsamples described in Sect. 4.

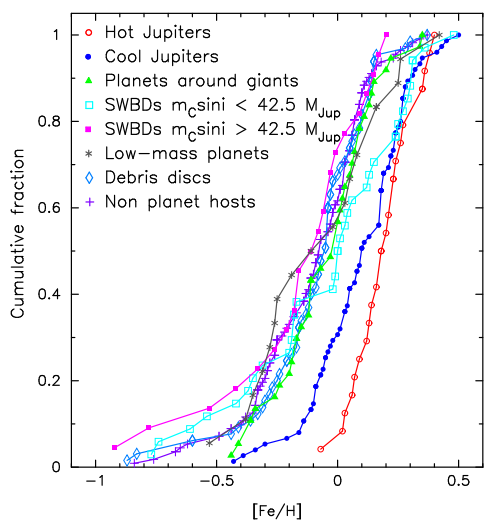


Fig. 4. $[\text{Fe}/\text{H}]$ cumulative frequencies for the different samples analysed in this work.

stellar objects, the range of the host star metallicities increases towards more negative values, suggesting that a non-metallicity

dependent formation mechanisms, such as gravitational instability or gravoturbulent fragmentation, might be at work.

In a recent work, Schlaufman (2018) computed the mass at which substellar companions no longer preferentially orbit metal-rich stars finding that while objects with masses below $10 M_{\text{Jup}}$ orbit metal-rich stars, substellar companions with masses larger than $10 M_{\text{Jup}}$ do not orbit metal-rich stars. We believe that our results are compatible with the findings by Schlaufman (2018) showing that the most massive substellar objects tend to form like stars.

Figure 6 shows the orbital period of the substellar companions as a function of the (minimum) mass of the substellar companions. Different colours indicate the eccentricity. The figure shows that the more massive substellar companions show larger periods and eccentricities ($P > 100$ days, $e > 0.05$). On the other hand, less massive companions have shorter periods and a wider range of eccentricities.

Setting together the trends from figures 5 and 6 it seems that as we move towards more massive planetary companions: *i*) their host stars show a wider (towards negative values) range of metallicities and higher stellar masses; *ii*) planets (or brown dwarfs) show longer periods and higher eccentricities. The differences in period and eccentricity distributions between both types of planets might be indicative of a different formation mechanism. In addition, the trend with the host star metallicity suggests that the higher the mass of the substellar companion, the higher the probability that it is formed by a non-metallicity dependent formation

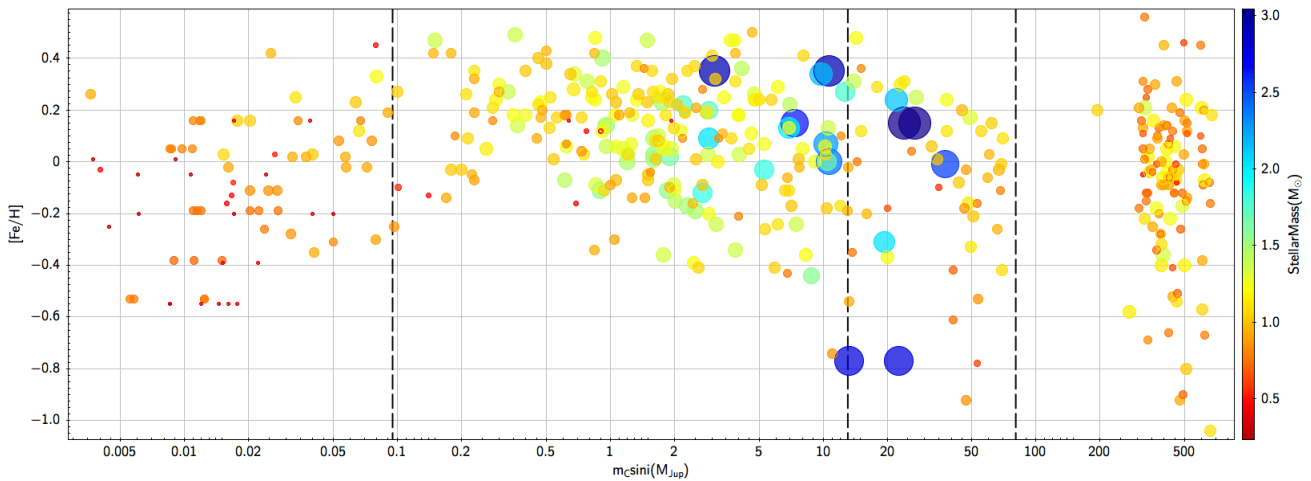


Fig. 5. Stellar metallicity of the host stars as a function of the minimum mass of the substellar companions. Different colours and symbol sizes indicate the mass of the host star. Vertical dashed lines indicate the standard mass loci of low-mass planets, gas-giant planets, brown dwarf, and stellar companions, from left to right respectively.

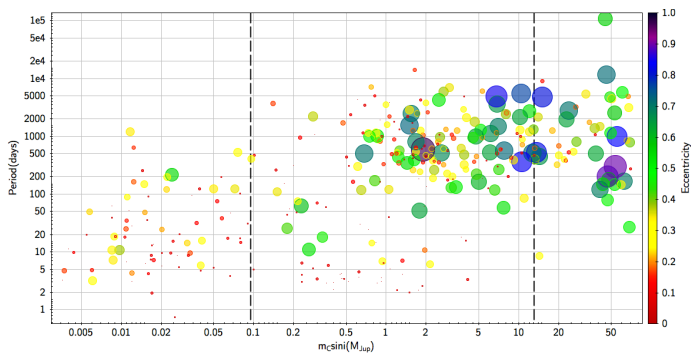


Fig. 6. Orbital period as a function of the minimum mass. Different colours and symbol sizes indicate the eccentricity values. Vertical dashed lines indicate the standard mass loci of low-mass planets, gas-giant planets, and brown dwarfs, from left to right.

mechanism. This general trend explain many of the correlations between the host star's metallicity and planetary properties discussed in recent works.

- *More massive stars host more massive planets.* It has been noticed that giant stars host more massive planets than their main-sequence counterparts (e.g. Johnson et al. 2007; Lovis & Mayor 2007; Maldonado et al. 2013), although this result should be taken with caution as the detection of small planets around evolved stars is hampered by the large levels of stellar jitter in these stars (e.g. Niedzielski et al. 2016). We note that in our sample, stars in the mass range $1.5\text{--}2 M_{\odot}$ host only planets with masses around $1 M_{\text{Jup}}$, while for stars more massive than $2 M_{\odot}$ planets are more massive than $2 M_{\text{Jup}}$. This trend might reflect a correlation between disc gas masses and giant planet masses (Alibert et al. 2011; Mordasini et al. 2012) as high-mass stars are likely to harbour more massive protoplanetary disk (e.g. Natta et al. 2000). In this scenario giant planet formation can occur in low metallicity but high-mass protoplanetary discs as it is the amount of metals in the disc the factor that drives the planet formation process (e.g. Ghezzi et al. 2018). The metallicity effect would depend on the mass of the disc, being the minimum metallicity required to form a massive planet lower for massive stars. Ghezzi et al. (2018) found that the relation between the

amount of metals in the protoplanetary disc and the formation of giant planets does almost follow a linear relationship. The lack of a clear planet-metallicity correlation found for giant stars might be explained by the fact that they host more massive planets and these planets might find a way in their more massive planetary discs to bypass the core-accretion mechanism and form more like stars. Finally, we note a tendency of more massive stars with substellar companions to have higher metallicities in agreement with previous works (Maldonado et al. 2013; Jofré et al. 2015).

- *Trends in brown dwarfs hosts.* Ma & Ge (2014); Mata Sánchez et al. (2014) showed that unlike gas-giant planet hosts, stars with brown dwarfs do not show metal-enrichment. Maldonado & Villaver (2017) found that stars with low-mass brown dwarfs tend to show higher metallicities than stars hosting more massive brown dwarfs. Ma & Ge (2014); Maldonado & Villaver (2017) also discussed differences in the period-eccentricity distribution of massive and low-mass brown dwarfs. This result fits well with our interpretation that more massive substellar objects tend to form more like stars.
- *Close-in and more distant planets.* Recent works (Sozzetti 2004; Maldonado et al. 2018; Wilson et al. 2018) have discussed whether hot Jupiters host stars show higher metallicities than more distant planets. As more distant planets are more massive than hot Jupiters (Ribas & Miralda-Escudé 2007; Bashi et al. 2017; Santos et al. 2017; Jenkins et al. 2017; Maldonado et al. 2018), see also Figure 6, they tend to orbit stars with a wider range of metallicities.
- *Planets around low-mass stars.* Planets around low-mass stars ($M_{\star} < 1 M_{\odot}$) are mainly low-mass planets and their host stars do not show metal enrichment. They have short periods and low eccentricities. On the other hand, very few gas-giant planets have been found orbiting around low-mass stars, showing their host stars metal-enrichment (Neves et al. 2013). We caution that these results refer to radial velocity planets. Results from transit surveys are discussed in Sect. 6.

We do not expect the general metallicity trends discussed in this work for massive planets and brown dwarfs to be severely affected by the different detection limits achieved for the different planet hosts. As discussed in Sect. 3 planets of the mass of Jupiter at short periods can be detected in more than 95% of

our targets. More distant substellar companions ($P > 100$ days) might be detected in a significant large percentage of our stars, between 60 and 80%. The possible trend between massive planetary companions and large periods might however be affected by our lower sensitivity to detect small gaseous planets (with masses of the order of the mass of Jupiter) at very long periods ($P > 2000$ days).

On the other hand, the results regarding low-mass planets should be regarded with caution as with the radial velocity data at hand, these planets can only be detected at short periods and around a small fraction of our stars (2 to 20% according to our conservative simulations, see Figure 2).

5. The planet-metallicity correlation in context

In order to discuss our results into a broader context, data from low-mass binaries have been included in Figure 5. The data is taken from Mann et al. (2013) who compiled the metallicity of the primary stars mainly from high-resolution spectra. The mass of the late-K, M companions as well as the primaries are estimated by using a spectral type - stellar mass relationship based on the data provided by Cox (2000).

The figure shows that the tendency of a wider range of metallicities (lower values) towards more massive objects continues in the low-mass stellar range. Despite the fact we are comparing the minimum mass of substellar objects with estimates of the mass of stars, the trend that more massive substellar or stellar objects tend to form in a non-metallicity dependent mechanism seems to hold, i.e., there seems to be a continuity between substellar and stellar companions. According to this figure the core-accretion mechanism for planet formation would have its highest efficiency for forming planets with masses around 1 Jupiter's mass (hot Jupiters).

It has been shown that the fraction of close binaries of solar-type stars decreases with the metallicity while the wide binary fraction is basically constant with metallicity at large separations (e.g. Moe et al. 2018; El-Badry & Rix 2018). Following the reasoning of Moe et al. (2018) massive and close substellar companions might form by fragmentation of the protostellar disc. Protostellar discs of solar-type stars are usually optically thick and lower metallicities imply lower opacities and enhanced cooling rates which translate in higher probabilities of disc fragmentation⁵. On the other hand, massive and distant companions might form by turbulent fragmentation of molecular cores, a process which is known to be independent of metallicity.

Figure 5 also reveals a possible tendency of wider metallicities towards low-mass planets which may still be formed by core-accretion around low-metallicity stars. The low-metallicity environment implies long times for forming a core able to accrete gas before the disc's dissipation, so only small planets and planetesimals can be formed (e.g. Mordasini et al. 2012). However, the sample of M dwarfs planet hosts is still too small to make a strong claim in these sense. We also should note our limited sensitivity to low-mass planet's detection. Debris disc's masses do not help either as they are usually unavailable and subject to many assumptions.

6. Comparison with Kepler results

Given that our planet host sample is mainly selected from radial velocity surveys a comparison with the results from the KEPLER

⁵ Although for very low metallicities, the disc becomes optically thin and the effect of lower metallicity would be the opposite.

mission is mandatory in order to achieve a full vision of planet formation.

In a recent work, Petigura et al. (2018) analyse a large sample of KEPLER objects of interest with metallicities derived from spectroscopic observations finding that planets smaller than Neptunes ($R_p < 4 R_\oplus$) are found around stars with a wide range of metallicities. On the other hand, sub-Saturns and Jupiters are found around metal-rich stars (their Figure 3). The authors also note a gradual upward trend in mean host star metallicity from smaller to larger planets in agreement with previous analysis of smaller samples (Buchhave et al. 2012, 2014). These results support our findings that only stars hosting Jupiter-like planets show preferentially the metal-rich signature. As lower planetary radius implies lower planetary masses, although the relationship is complex and depend on the planet composition (e.g. Lopez & Fortney 2014), we conclude that the KEPLER data supports our suggestion that a tendency of lower metallicities towards low-mass planets might be hidden in Fig. 5 as discussed in Sect. 5.

Similar results have been found by Narang et al. (2018) who show that the host star metallicity, increases with larger planetary radius/mass up to about $1 M_{Jup}$ or $4 R_\oplus$. For planetary masses larger than $4 M_{Jup}$ the authors also found that more massive planets have on average lower host star metallicities in agreement with our findings. The authors also discuss that hot transiting planets (periods less than 10 days) orbit around stars with higher average metallicity in agreement with our previous results (Maldonado et al. 2018) and this work.

Studies of the KEPLER occurrence rates (Mulders et al. 2015a,b) have confirmed that small planets ($1.0 - 3.0 R_\oplus$) are more common around M dwarfs than around main-sequence FGK stars (Howard et al. 2012). At larger planetary radii planets become more common around sun-like stars. Despite begin different samples ($1.0 - 3.0 R_\oplus$ planets correspond to masses below $\sim 8 M_\oplus$, i.e., planets smaller than Neptune), a similar tendency of a larger occurrence of small planets towards less massive stars is found in our results from Fig. 5 where it can be seen that the vast majority of the low-mass planets ($m_c \sin i < 30 M_\oplus$) orbit around stars with masses below $1 M_\odot$.

7. Conclusions

Achieving a full vision of how planets and planetary systems form and evolve is only possible by analysing in a homogeneous way large samples of stars covering the full domain of parameters, i.e, including the different outcomes of the planet formation process (from planetesimals to massive brown dwarfs and low-mass stars) as well as the full range of host star's masses and types. In this work we performed a detailed analysis of the planet-metallicity correlation by analysing in a joined way the data from our previous works, focused on certain types of stars and/or planets. Most of the studied stars (excluding the M dwarf subsample) was analysed in the same way using similar spectra and techniques.

Our results show a continuity between the formation of substellar and stellar companions driven by the metallicity of the host star. The core-accretion formation mechanism would achieve its maximum efficiency for planets with masses between ~ 0.2 and $2 M_{Jup}$. For more massive substellar objects as well in low-mass binary companions the range of host star's metallicities increases towards lower values, suggesting that both kind of objects tend to share similar formation mechanisms.

Another tendency towards lower host star's metallicities seems to be present towards the less massive outcomes of the

planet formation process (low-mass planets and probably planetesimals) which may still be formed by the core-accretion method. However, this tendency might need additional confirmation.

Acknowledgements. This research was supported by the Italian Ministry of Education, University, and Research through the *PREMIALE WOW 2013* research project under grant *Ricerca di pianeti intorno a stelle di piccola massa*. J. M. acknowledges support from the Ariel ASI-INAF agreement N. 2015-038-R.0. E. V., and C. E. acknowledge support from the *On the rocks* project funded by the Spanish Ministerio de Economía y Competitividad under grant *AYA2014-55840-P*. We sincerely appreciate the careful reading of the manuscript and the constructive comments of an anonymous referee.

References

- Alibert, Y., Mordasini, C., & Benz, W. 2011, *A&A*, 526, A63
- Bashi, D., Helled, R., Zucker, S., & Mordasini, C. 2017, *A&A*, 604, A83
- Beichman, C. A., Bryden, G., Rieke, G. H., et al. 2005, *ApJ*, 622, 1160
- Bouchy, F., Ségransan, D., Díaz, R. F., et al. 2016, *A&A*, 585, A46
- Bressan, A., Marigo, P., Girardi, L., et al. 2012, *MNRAS*, 427, 127
- Bryden, G., Beichman, C. A., Carpenter, J. M., et al. 2009, *ApJ*, 705, 1226
- Buchhave, L. A., Bizzarro, M., Latham, D. W., et al. 2014, *Nature*, 509, 593
- Buchhave, L. A. & Latham, D. W. 2015, *ApJ*, 808, 187
- Buchhave, L. A., Latham, D. W., Johansen, A., et al. 2012, *Nature*, 486, 375
- Chavero, C., Gómez, M., Whitney, B. A., & Saffe, C. 2006, *A&A*, 452, 921
- Cox, A. N. 2000, *Allen's astrophysical quantities*
- Cumming, A. & Dragomir, D. 2010, *MNRAS*, 401, 1029
- da Silva, L., Girardi, L., Pasquini, L., et al. 2006, *A&A*, 458, 609
- El-Badry, K. & Rix, H.-W. 2018, *ArXiv e-prints* [[arXiv:1809.06860](https://arxiv.org/abs/1809.06860)]
- Endl, M., Kürster, M., Els, S., Hatzes, A. P., & Cochran, W. D. 2001, *A&A*, 374, 675
- Endl, M., Kürster, M., Els, S., et al. 2002, *A&A*, 392, 671
- ESA, ed. 1997, *ESA Special Publication*, Vol. 1200, *The HIPPARCOS and TYCHO catalogues. Astrometric and photometric star catalogues derived from the ESA HIPPARCOS Space Astrometry Mission*
- Fischer, D. A., Laughlin, G., Butler, P., et al. 2005, *ApJ*, 620, 481
- Fischer, D. A. & Valenti, J. 2005, *ApJ*, 622, 1102
- Galland, F., Lagrange, A. M., Udry, S., et al. 2005, *A&A*, 443, 337
- Gáspár, A., Rieke, G. H., & Ballering, N. 2016, *ApJ*, 826, 171
- Ghezzi, L., Cunha, K., Schuler, S. C., & Smith, V. V. 2010a, *ApJ*, 725, 721
- Ghezzi, L., Cunha, K., Smith, V. V., et al. 2010b, *ApJ*, 720, 1290
- Ghezzi, L., Montet, B. T., & Johnson, J. A. 2018, *ApJ*, 860, 109
- Girardi, L., Bressan, A., Bertelli, G., & Chiosi, C. 2000, *A&AS*, 141, 371
- Gonzalez, G. 1997, *MNRAS*, 285, 403
- Greaves, J. S., Fischer, D. A., & Wyatt, M. C. 2006, *MNRAS*, 366, 283
- Hekker, S. & Meléndez, J. 2007, *A&A*, 475, 1003
- Hekker, S., Reffert, S., Quirrenbach, A., et al. 2006, *A&A*, 454, 943
- Howard, A. W., Marcy, G. W., Bryson, S. T., et al. 2012, *ApJS*, 201, 15
- Jenkins, J. S., Jones, H. R. A., Tuomi, M., et al. 2017, *MNRAS*, 466, 443
- Jofré, E., Petrucci, R., Saffe, C., et al. 2015, *A&A*, 574, A50
- Johnson, J. A., Fischer, D. A., Marcy, G. W., et al. 2007, *ApJ*, 665, 785
- Kokubo, E. & Ida, S. 2002, *ApJ*, 581, 666
- Kóspál, Á., Ardila, D. R., Moór, A., & Ábrahám, P. 2009, *ApJ*, 700, L73
- Lagrange, A. M., De Bondt, K., Meunier, N., et al. 2012, *A&A*, 542, A18
- Lopez, E. D. & Fortney, J. J. 2014, *ApJ*, 792, 1
- Lovis, C. & Mayor, M. 2007, *A&A*, 472, 657
- Ma, B. & Ge, J. 2014, *MNRAS*, 439, 2781
- Maldonado, J., Affer, L., Micela, G., et al. 2015a, *A&A*, 577, A132
- Maldonado, J., Eiroa, C., Villaver, E., Montesinos, B., & Mora, A. 2012, *A&A*, 541, A40
- Maldonado, J., Eiroa, C., Villaver, E., Montesinos, B., & Mora, A. 2015b, *A&A*, 579, A20
- Maldonado, J. & Villaver, E. 2016, *A&A*, 588, A98
- Maldonado, J. & Villaver, E. 2017, *A&A*, 602, A38
- Maldonado, J., Villaver, E., & Eiroa, C. 2013, *A&A*, 554, A84
- Maldonado, J., Villaver, E., & Eiroa, C. 2018, *A&A*, 612, A93
- Mann, A. W., Brewer, J. M., Gaidos, E., Lépine, S., & Hilton, E. J. 2013, *AJ*, 145, 52
- Mata Sánchez, D., González Hernández, J. I., Israelian, G., et al. 2014, *A&A*, 566, A83
- Mayor, M., Marmier, M., Lovis, C., et al. 2011, *ArXiv e-prints* [[arXiv:1109.2497](https://arxiv.org/abs/1109.2497)]
- Meunier, N., Lagrange, A. M., & De Bondt, K. 2012, *A&A*, 545, A87
- Moe, M., Kratter, K. M., & Badenes, C. 2018, *ArXiv e-prints* [[arXiv:1808.02116](https://arxiv.org/abs/1808.02116)]
- Mordasini, C., Alibert, Y., Benz, W., Klahr, H., & Henning, T. 2012, *A&A*, 541, A97
- Mortier, A., Santos, N. C., Sousa, S. G., et al. 2013, *A&A*, 557, A70
- Mulders, G. D., Pascucci, I., & Apai, D. 2015a, *ApJ*, 798, 112
- Mulders, G. D., Pascucci, I., & Apai, D. 2015b, *ApJ*, 814, 130
- Narang, M., Manoj, P., Furlan, E., et al. 2018, *AJ*, 156, 221
- Natta, A., Grinin, V., & Mannings, V. 2000, *Protostars and Planets IV*, 559
- Neves, V., Bonfils, X., Santos, N. C., et al. 2013, *A&A*, 551, A36
- Niedzielski, A., Deka-Szymankiewicz, B., Adamczyk, M., et al. 2016, *A&A*, 585, A73
- Niedzielski, A., Nowak, G., Adamów, M., & Wolszczan, A. 2009, *ApJ*, 707, 768
- Niedzielski, A. & Wolszczan, A. 2008, in *Astronomical Society of the Pacific Conference Series*, Vol. 398, *Extreme Solar Systems*, ed. D. Fischer, F. A. Rasio, S. E. Thorsett, & A. Wolszczan, 71
- Pasquini, L., Döllinger, M. P., Weiss, A., et al. 2007, *A&A*, 473, 979
- Pepe, F., Mayor, M., Queloz, D., et al. 2004, *A&A*, 423, 385
- Petigura, E. A., Marcy, G. W., Winn, J. N., et al. 2018, *AJ*, 155, 89
- Pollack, J. B., Hubickyj, O., Bodenheimer, P., et al. 1996, *Icarus*, 124, 62
- Reffert, S., Bergmann, C., Quirrenbach, A., Trifonov, T., & Künstler, A. 2015, *A&A*, 574, A116
- Ribas, I. & Miralda-Escudé, J. 2007, *A&A*, 464, 779
- Sadakane, K., Ohnishi, T., Ohkubo, M., & Takeda, Y. 2005, *PASJ*, 57, 127
- Sahlmann, J., Ségransan, D., Queloz, D., et al. 2011, *A&A*, 525, A95
- Santos, N. C., Adibekyan, V., Figueira, P., et al. 2017, *A&A*, 603, A30
- Santos, N. C., Israelian, G., & Mayor, M. 2004, *A&A*, 415, 1153
- Schlaufman, K. C. 2018, *ApJ*, 853, 37
- Schuler, S. C., Kim, J. H., Tinker, Jr., M. C., et al. 2005, *ApJ*, 632, L131
- Sousa, S. G., Santos, N. C., Israelian, G., Mayor, M., & Udry, S. 2011, *A&A*, 533, A141
- Sozzetti, A. 2004, *MNRAS*, 354, 1194
- Takeda, Y., Ohkubo, M., Sato, B., Kambe, E., & Sadakane, K. 2005, *PASJ*, 57, 27
- Takeda, Y., Sato, B., & Murata, D. 2008, *PASJ*, 60, 781
- Tinney, C. G., Butler, R. P., Marcy, G. W., et al. 2001, *ApJ*, 551, 507
- van Leeuwen, F. 2007, *A&A*, 474, 653
- Wilson, P. A., Hébrard, G., Santos, N. C., et al. 2016, *A&A*, 588, A144
- Wilson, R. F., Teske, J., Majewski, S. R., et al. 2018, *AJ*, 155, 68
- Wright, J. T. & Howard, A. W. 2009, *ApJS*, 182, 205

Appendix A: Additional tables

Table A.1. Basic properties of the stars considered in this work.

HIP/Other	HD	V (mag)	SpType	[Fe/H] (dex)	M _★ (M _☉)	Ref [†]	Sample/Notes
171	224930	5.80	G3V	-0.83 ± 0.01	0.68 ± 0.00	1	Debris disc
439	225213	8.60	M2.5	-0.27 ± 0.09	0.33 ± 0.07	5	M dwarf, comparison
490	105	7.51	G0V	-0.16 ± 0.03	0.99 ± 0.02	1	Debris disc
522	142	5.70	G1IV	0.07 ± 0.02	1.25 ± 0.01	4	Debris disc and two planets
544	166	6.07	K0V	0.15 ± 0.02	1.00 ± 0.01	1	Debris disc
729	448	5.57	G9III	0.04 ± 0.04	1.81 ± 0.08	2	Giant star, comparison sample
873	645	5.84	K0III	0.03 ± 0.02	1.78 ± 0.05	2	Giant star, comparison sample
910	693	4.89	F5V	-0.40 ± 0.01	1.02 ± 0.01	1	Comparison sample
1292	1237	6.59	G6V	0.11 ± 0.02	0.98 ± 0.01	4	Cool planet
1499	1461	6.47	G0V	0.16 ± 0.03	1.05 ± 0.02	1	Debris disc and two low-mass planets
1598	1562	6.97	G0	-0.27 ± 0.02	0.88 ± 0.02	1	Debris disc
1599	1581	4.23	F9V	-0.24 ± 0.02	0.92 ± 0.01	1	Debris disc
1692	1690	9.17	K1III	-0.24 ± 0.04	1.11 ± 0.15	2	Giant star, planet host
1931	2039	9.00	G2/G3IV/V	0.29 ± 0.02	1.20 ± 0.04	4	Cool planet
2350	2638	9.44	G5	0.20 ± 0.02	0.92 ± 0.02	4	Hot planet
2941	3443	5.57	K1V	-0.12 ± 0.03	0.91 ± 0.01	1	Comparison sample
3093	3651	5.88	K0V	0.19 ± 0.02	0.92 ± 0.02	1	Two cool planets
3170	3823	5.89	G1V	-0.34 ± 0.01	0.95 ± 0.01	1	Comparison sample
3185	3795	6.14	G3/G5V	-0.67 ± 0.01	0.87 ± 0.00	1	Comparison sample
3497	4308	6.55	G3V	-0.35 ± 0.01		1	Low-mass planet
3559	4307	6.15	G2V	-0.33 ± 0.01	0.97 ± 0.01	1	Comparison sample
3765	4628	5.74	K2V	-0.23 ± 0.03	0.76 ± 0.02	1	Comparison sample
3821	4614	3.46	G0V	-0.28 ± 0.01	0.89 ± 0.01	1	Comparison sample
3850	4747	7.15	G8/K0V	-0.18 ± 0.02	0.85 ± 0.01	3	High-mass brown dwarf
3909	4813	5.17	F7IV-V	-0.13 ± 0.01	1.07 ± 0.01	1	Comparison sample
4148	5133	7.15	K2V	-0.12 ± 0.03	0.77 ± 0.02	1	Debris disc
4297	5319	8.05	G5IV	0.05 ± 0.03	1.30 ± 0.07	2	Giant star, two planets
4311	5388	6.73	F6V	-0.42 ± 0.01	1.10 ± 0.02	3	High-mass brown dwarf
5158		10.16	K5	0.36 ± 0.04	0.80 ± 0.02	3	Low-mass brown dwarf + planet
5336	6582	5.17	G5V	-0.87 ± 0.01		1	Debris disc
5862	7570	4.97	F8V	0.10 ± 0.02	1.15 ± 0.01	1	Debris disc
5944	7590	6.59	G0	-0.08 ± 0.03	1.04 ± 0.02	1	Debris disc
6379	7924	7.17	K0	-0.11 ± 0.03	0.84 ± 0.01	1	Three low-mass planets
6512	8375	6.28	G8IV	-0.09 ± 0.01	1.55 ± 0.02	2	Giant star, comparison sample
6682	8594	7.25	K0	0.00 ± 0.03	1.31 ± 0.07	2	Giant star, comparison sample
6999	9057	5.27	K0III	0.07 ± 0.03	2.43 ± 0.08	2	Giant star, comparison sample
7097	9270	3.62	G8III	-0.09 ± 0.06	3.62 ± 0.14	2	Giant star, comparison sample
7513	9826	4.10	F8V	0.06 ± 0.02	1.26 ± 0.04	4	Three planets
7576	10008	7.66	G5	-0.02 ± 0.03	0.89 ± 0.02	1	Debris disc
7607	9927	3.59	K3III	0.11 ± 0.07	1.85 ± 0.20	2	Giant star, comparison sample
7719	10072	5.01	G8III	-0.12 ± 0.02	2.32 ± 0.10	2	Giant star, comparison sample
7978	10647	5.52	F8V	-0.11 ± 0.03	1.08 ± 0.02	1	Debris disc and planet
7981	10476	5.24	K1V	0.03 ± 0.02	0.89 ± 0.01	1	Comparison sample
8102	10700	3.49	G8V	-0.53 ± 0.01	0.78 ± 0.01 [‡]	1	Debris disc and 4 low-mass planets
8159	10697	6.27	G5IV	0.12 ± 0.03	1.11 ± 0.02	3	Subgiant, low-mass brown dwarf
8486	11131	6.72	G0	-0.08 ± 0.01	1.01 ± 0.02	1	Comparison sample
8770	11506	7.51	G0V	0.25 ± 0.02	1.22 ± 0.01	4	Two planets
9222	11949	5.70	K0IV	-0.15 ± 0.02	1.52 ± 0.04	2	Giant star, comparison sample
9683	12661	7.43	K0	0.35 ± 0.02	1.09 ± 0.01	4	Two planets
10085	13189	7.57	K2	-0.37 ± 0.05	1.23 ± 0.25	3	Giant star, low-mass brown dwarf
10138	13445	6.12	K0V	-0.21 ± 0.02	0.79 ± 0.02	1	Cool planet
10279		10.10	M2	-0.16 ± 0.09	0.43 ± 0.06	5	M dwarf, comparison
10306	13555	5.23	F5V	-0.25 ± 0.03	1.29 ± 0.04	1	Comparison sample
10321	13507	7.19	G0	-0.03 ± 0.02	0.99 ± 0.02	3	High-mass brown dwarf
10798	14412	6.33	G8V	-0.49 ± 0.01	0.73 ± 0.01	1	Comparison sample
10868	14348	7.19	F5	0.17 ± 0.02	1.31 ± 0.02	3	Subgiant, High-mass brown dwarf
11028	14651	8.26	G0	-0.03 ± 0.01	0.89 ± 0.02	3	High-mass brown dwarf
11072	14802	5.19	G2V	-0.07 ± 0.01	1.12 ± 0.01	1	Comparison sample
12048	16141	6.83	G5IV	0.09 ± 0.01	1.08 ± 0.01	4	Subgiant, planet host

Table A.1. Continued.

HIP/Other	HD	V (mag)	SpType	[Fe/H] (dex)	M_{\star} (M_{\odot})	Ref [†]	Sample/Notes
12114	16160	5.79	K3V	-0.10 ± 0.05	0.76 ± 0.02	1	Comparison sample
12191	16175	7.28	G0	0.26 ± 0.02	1.31 ± 0.03	2	Subgiant star, planet host
12247	16400	5.65	G5III	-0.03 ± 0.03	1.83 ± 0.09	2	Giant star, planet host
12350	16548	6.98	G0	0.10 ± 0.01	1.19 ± 0.03	2	Subgiant star, comparison sample
12638	16760	8.70	G5	-0.02 ± 0.01	0.95 ± 0.02	3	Low-mass brown dwarf
12777	16895	4.10	F7V	-0.04 ± 0.03	1.16 ± 0.02	1	Comparison sample
	17092	7.73		0.11 ± 0.05	1.23 ± 0.18	2	Giant star, planet host
13402	17925	6.05	K1V	0.10 ± 0.03	0.89 ± 0.01	1	Debris disc
13531	17878	3.93	G4III	-0.20 ± 0.03	2.91 ± 0.08	2	Giant star, comparison sample
13642	18143	7.52	K2	0.28 ± 0.05	0.91 ± 0.03	1	Debris disc
14086	18907	5.88	G8/K0V	-0.68 ± 0.01		2	Subgiant star, comparison sample
14632	19373	4.05	G0V	0.09 ± 0.01	1.12 ± 0.01	1	Comparison sample
14954	19994	5.07	F8V	0.10 ± 0.04	1.32 ± 0.03	4	Debris disc and planet
15330	20766	5.53	G2V	-0.22 ± 0.02	0.91 ± 0.02	1	Comparison sample
15371	20807	5.24	G1V	-0.28 ± 0.01	0.88 ± 0.01	1	Debris disc
15457	20630	4.84	G5V	0.09 ± 0.02	1.04 ± 0.01	1	Comparison sample
15510	20794	4.26	G8V	-0.38 ± 0.02	0.70 [‡]	1	Debris disc and 3 low-mass planets
15527	20782	7.36	G3V	-0.10 ± 0.02	0.93 ± 0.01	4	Cool planet
15776	21019	6.20	G2V	-0.56 ± 0.01	1.01 ± 0.02	2	Subgiant star, comparison sample
16537	22049	3.72	K2V	-0.04 ± 0.02	0.83±0.05 [‡]	4	Debris disc and planet
16852	22484	4.29	F9V	-0.11 ± 0.01	1.09 ± 0.01	1	Debris disc
17096	23079	7.12	F8/G0V	-0.16 ± 0.01	0.97 ± 0.01	4	Cool planet
17183	22918	6.96	G5	-0.01 ± 0.02	1.07 ± 0.03	2	Subgiant star, comparison sample
17187	22781	8.78	K0	-0.35 ± 0.02	0.75 ± 0.02	3	Low-mass brown dwarf
17378	23249	3.52	K0IV	0.08 ± 0.02	1.17 ± 0.01	2	Subgiant star, comparison sample
17420	23356	7.10	K2V	-0.05 ± 0.03	0.80 ± 0.02	1	Debris disc
18432	24892	6.88	G8V	-0.38 ± 0.01	0.93 ± 0.02	2	Subgiant star, comparison sample
19038	25604	4.36	K0III	0.09 ± 0.04	2.24 ± 0.12	2	Giant star, comparison sample
19849	26965	4.43	K1V	-0.26 ± 0.02	0.76 ± 0.01	1	Comparison sample
19855	26913	6.94	G5IV	-0.03 ± 0.02	0.98 ± 0.01	1	Comparison sample
20199	27631	8.26	G3IV/V	-0.14 ± 0.01	0.90 ± 0.01	4	Cool planet
GSC02883-01687		12.16	G5	0.32 ± 0.03	1.05 ± 0.01	2	Hot planet
20723	28185	7.80	G5	0.24 ± 0.02	1.05 ± 0.01	4	Cool planet
20834	283668	9.40	K3V	-0.78 ± 0.01	0.62 ± 0.01	3	High-mass brown dwarf
20889	28305	3.53	K0 III	0.15 ± 0.04	2.63 ± 0.07	2	Giant star, planet host
21832	29587	7.29	G2V	-0.61 ± 0.01	0.74 ± 0.00	3	Low-mass brown dwarf
21850	30177	8.41	G8V	0.41 ± 0.02	1.07 ± 0.01	4	Two cool planets
21932	285968	10.00	M2	0.03 ± 0.09	0.52 ± 0.05	5	M dwarf, low-mass planet
22203	30246	8.30	G5	0.12 ± 0.01	1.07 ± 0.01	3	High-mass brown dwarf
22263	30495	5.49	G3V	0.01 ± 0.01	1.05 ± 0.01	1	Debris disc
22320	30669	9.12	G8/K0V	0.17 ± 0.02	0.96 ± 0.02	4	Cool planet
23311	32147	6.22	K3V	0.37 ± 0.05	0.83 ± 0.02	1	Comparison sample
23816	33081	7.04	F7V	-0.19 ± 0.05	1.16 ± 0.04	1	Debris disc
23889	33283	8.05	G3/G5V	0.27 ± 0.02	1.39 ± 0.04	4	Cool planet
24186	33793	8.80	M0	-0.39 ± 0.09	0.35 ± 0.05	5	M dwarf, two low-mass planets
24205	33636	7.00	G0	-0.16 ± 0.01	0.98 ± 0.01	1	Debris disc
24786	34721	5.96	G0V	0.05 ± 0.04	1.15 ± 0.02	1	Comparison sample
24813	34411	4.69	G0V	0.07 ± 0.01	1.06 ± 0.01	1	Comparison sample
25110	33564	5.08	F6V	0.00 ± 0.04	1.27 ± 0.02	1	Cool planet
25878	36395	8.00	M1.5	0.00 ± 0.09	0.60 ± 0.06	5	M dwarf, planet host
26394	39091	5.65	G3IV	0.03 ± 0.01	1.07 ± 0.01	3	Low-mass brown dwarf and planet
26779	37394	6.21	K1V	0.16 ± 0.02	0.93 ± 0.00	1	Debris disc
27072	38393	3.59	F7V	-0.05 ± 0.03	1.20 ± 0.02	1	Debris disc
27253	38529	5.95	G4V	0.31 ± 0.04	1.38 ± 0.02	3	Subgiant, low-mass BD and planet
27435	38858	5.97	G4V	-0.25 ± 0.01	0.87 ± 0.01	1	Debris disc and low-mass planet
27828	39392	8.40	F8	-0.54 ± 0.01	0.94 ± 0.04	3	Low-mass brown dwarf
27887	40307	7.17	K3V	-0.19 ± 0.04	0.74 ± 0.02	1	Debris disc and 6 low-mass planets
27913	39587	4.39	G0V	0.01 ± 0.03	1.07 ± 0.00	1	Comparison sample
27980	39833	7.65	G0III	0.15 ± 0.02	1.09 ± 0.02	1	Debris disc
28393	41004	8.65	K2V	0.21 ± 0.03	0.92 ± 0.02	4	Cool planet

Table A.1. Continued.

HIP/Other	HD	V (mag)	SpType	[Fe/H] (dex)	M_{\star} (M_{\odot})	Ref [†]	Sample/Notes
28767	40979	6.74	F8	0.18 ± 0.02	1.24 ± 0.01	1	Debris disc and planet
28954	41593	6.76	K0	0.03 ± 0.03	0.89 ± 0.01	1	Comparison sample
29271	43834	5.08	G5V	0.13 ± 0.02	1.00 ± 0.02	1	Debris disc
29295	42581	8.20	M1	-0.10 ± 0.09	0.55 ± 0.05	5	M dwarf, brown dwarf + low-mass planet
29568	43162	6.37	G5V	0.01 ± 0.03	0.98 ± 0.01	1	Comparison sample
30503	45184	6.37	G2V	0.03 ± 0.01	1.03 ± 0.01	1	Debris disc and low-mass planet
31246	46375	7.91	K1IV	0.32 ± 0.03	0.94 ± 0.02	4	Debris disc and planet
31293		10.50	M3	-0.04 ± 0.09	0.45 ± 0.06	5	M dwarf, comparison
31592	47205	3.95	K1III	-0.39 ± 0.09	1.23 ± 0.12	4	Cool planet
31711	48189	6.15	G1/G2V	-0.17 ± 0.06	0.97 ± 0.04	1	Debris disc
32439	46588	5.44	F8V	-0.14 ± 0.02	1.06 ± 0.02	1	Comparison sample
32480	48682	5.24	G0V	0.09 ± 0.02	1.16 ± 0.01	1	Debris disc
32916	49674	8.10	G0	0.27 ± 0.02	1.05 ± 0.02	4	Hot planet
32970	50499	7.21	G1V	0.27 ± 0.02	1.23 ± 0.01	4	Debris disc and planet
32984	50281	6.58	K3V	0.01 ± 0.05	0.75 ± 0.02	1	Comparison sample
	50281B	10.10	M2.5	-0.13 ± 0.09	0.44 ± 0.06	5	M dwarf, comparison
33212	50554	6.84	F8	-0.09 ± 0.01	1.03 ± 0.01	1	Debris disc and planet
33277	50692	5.74	G0V	-0.21 ± 0.02	0.93 ± 0.02	1	Comparison sample
33690	53143	6.81	K0IV-V	0.15 ± 0.03	0.97 ± 0.01	1	Debris disc
33719	52265	6.29	G0III-IV	0.18 ± 0.02	1.21 ± 0.01	4	Debris disc and 2 planets
34017	52711	5.93	G4V	-0.14 ± 0.02	0.96 ± 0.01	1	Comparison sample
34065	53705	5.56	G3V	-0.25 ± 0.01	0.89 ± 0.01	1	Comparison sample
35136	55575	5.54	G0V	-0.38 ± 0.02	0.89 ± 0.01	1	Comparison sample
36208		9.80	M4	0.01 ± 0.09	0.27 ± 0.12	5	M dwarf, 2 low-mass planets
36439	58855	5.35	F6V	-0.33 ± 0.03	1.05 ± 0.02	1	Comparison sample
36616	59686	5.45	K2III	0.13 ± 0.04	1.98 ± 0.19	2	Giant star, planet host
36795	60532	4.45	F6IV-V	-0.24 ± 0.02	1.36 ± 0.01	2	Subgiant star, two planets
36827	60491	8.16	K2V	-0.21 ± 0.04	0.78 ± 0.02	1	Debris disc
36906	60234	7.68	G0	0.03 ± 0.03	1.54 ± 0.08	1	Debris disc
NGC2423-3		10.04	G5IV-V/K2III	0.00 ± 0.04	2.40 ± 0.20 ^{a)}	3	Low-mass brown dwarf
37826	62509	1.15	K0III	0.09 ± 0.03	2.03 ± 0.07	2	Giant star, planet host
37853	63077	5.36	G0V	-0.84 ± 0.01		1	Comparison sample
38558	65216	7.97	G5V	-0.14 ± 0.02	0.92 ± 0.02	4	Two cool planets
38784	62613	6.55	G8V	-0.09 ± 0.02	0.92 ± 0.02	1	Comparison sample
39064	65430	7.68	K0V	-0.11 ± 0.02	0.80 ± 0.01	3	High-mass brown dwarf
39903	68456	4.74	F5V	-0.34 ± 0.06	1.19 ± 0.05	1	Comparison sample
40501		10.10	M2	-0.17 ± 0.09	0.43 ± 0.05	5	M dwarf, comparison
40693	69830	5.95	K0V	0.02 ± 0.04	0.93 ± 0.02	4	Debris disc and 3 low-mass planets
40843	69897	5.13	F6V	-0.32 ± 0.02	1.03 ± 0.01	1	Comparison sample
41484	71148	6.32	G5V	0.03 ± 0.02	1.04 ± 0.02	1	Comparison sample
41926	72673	6.38	K0V	-0.33 ± 0.02	0.76 ± 0.02	1	Comparison sample
42074	72760	7.32	G5	0.06 ± 0.02	0.93 ± 0.01	1	Comparison sample
42173	72946	7.25	G5V	0.03 ± 0.02	0.96 ± 0.07 ^{b)}	3	High-mass brown dwarf
42214	73256	8.08	G8/K0V	0.26 ± 0.02	1.03 ± 0.02	4	Hot planet
42282	73526	8.99	G6V	0.19 ± 0.02	1.06 ± 0.04	1	Debris disc and two planets
42333	73350	6.74	G0	0.13 ± 0.02	1.09 ± 0.01	1	Debris disc
42430	73752	5.05	G3/G5V	0.26 ± 0.04	1.26 ± 0.04	1	Comparison sample
42438	72905	5.63	G1.5V	-0.02 ± 0.03	1.05 ± 0.00	1	Debris disc
42446	73534	8.23	G5	0.29 ± 0.05	1.25 ± 0.05	4	Subgiant star, planet host
HAT-P-13		10.62	G4	0.48 ± 0.03	1.22 ± 0.03	3	Low-mass brown dwarf and planet
42527	73108	5.79	K1III	-0.17 ± 0.03	1.01 ± 0.04	2	Giant star, planet host
42528	73764	6.60	K0	0.01 ± 0.03	1.76 ± 0.05	2	Giant star, comparison sample
42723	74156	7.61	G0	0.05 ± 0.02	1.21 ± 0.04	4	Two cool planets
42808	74576	6.58	K2V	0.05 ± 0.03	0.83 ± 0.01	1	Comparison sample
43177	75289	6.35	G0	0.23 ± 0.02	1.23 ± 0.01	4	Hot planet
43587	75732	5.96	G8V	0.42 ± 0.03	0.98 ± 0.01	1	Four giant, one low-mass planets
43625	75616	6.92	F5	-0.36 ± 0.03	1.01 ± 0.03	1	Debris disc
43686	76700	8.16	G8V	0.35 ± 0.02	1.13 ± 0.08	4	Hot planet
43726	76151	6.01	G3V	0.13 ± 0.02	1.08 ± 0.01	1	Debris disc
44259	77065	8.78	G5	-0.42 ± 0.02	0.71 ± 0.01	3	Low-mass brown dwarf

Table A.1. Continued.

HIP/Other	HD	V (mag)	SpType	[Fe/H] (dex)	M_{\star} (M_{\odot})	Ref [†]	Sample/Notes
44291	77338	8.63	K0IV	0.38 ± 0.03	1.00 ± 0.01	4	Hot planet
44387		9.95	K7	0.04 ± 0.04	0.77 ± 0.02	3	Low-mass brown dwarf
44897	78366	5.95	F9V	0.00 ± 0.02	1.04 ± 0.02	1	Comparison sample
45333	79028	5.18	F9V	0.07 ± 0.03	1.14 ± 0.03	1	Comparison sample
45617	79969	7.20	K3V	-0.08 ± 0.05	0.79 ± 0.00	1	Comparison sample
45908	304636	9.50	M0.5	-0.16 ± 0.09	0.53 ± 0.05	5	M dwarf, comparison
46471	81688	5.41	K0III-IV	-0.36 ± 0.02	1.33 ± 0.22	2	Giant star, planet host
46580	82106	7.20	K3V	0.02 ± 0.05	0.77 ± 0.02	1	Comparison sample
47007	82943	6.54	G0	0.24 ± 0.01	1.17 ± 0.01	4	Debris disc and 3 planets
47103		10.90	M2.5	-0.27 ± 0.09	0.32 ± 0.07	5	M dwarf, comparison
47202	83443	8.23	K0V	0.35 ± 0.02	1.02 ± 0.01	4	Hot planet
47425		10.80	M3	0.04 ± 0.09	0.42 ± 0.08	5	M dwarf, comparison
47592	84117	4.93	G0V	-0.07 ± 0.04	1.07 ± 0.02	1	Comparison sample
47780		10.10	M2.5	-0.06 ± 0.09	0.46 ± 0.06	5	M dwarf, comparison
48113	84737	5.08	G2V	0.11 ± 0.02	1.16 ± 0.04	1	Comparison sample
48711	86081	8.73	F8	0.16 ± 0.02	1.19 ± 0.04	4	Hot planet
48739	86226	7.93	G2V	-0.05 ± 0.01	1.00 ± 0.01	4	Two cool planets
48780	86264	7.41	F7V	0.22 ± 0.05	1.41 ± 0.03	4	Cool planet
49081	86728	5.37	G1V	0.24 ± 0.02	1.10 ± 0.01	1	Comparison sample
49699	87883	7.56	K0	0.10 ± 0.05	0.83 ± 0.02	1	Cool planet
49813	88133	8.01	G5 IV	0.30 ± 0.02	1.24 ± 0.05	2	Subgiant star, planet host
49986		9.30	M2	-0.01 ± 0.09	0.53 ± 0.05	5	M dwarf, planet host
BD+202457		9.75	K2II	-0.77 ± 0.03	$2.8 \pm 1.5^{\text{c}}$	3	Giant star, two low-mass brown dwarfs
50384	89125	5.81	F8V	-0.41 ± 0.02	0.94 ± 0.01	1	Debris disc
GJ388		9.40	M3.5	0.12 ± 0.10	0.47 ± 0.07	5	M dwarf, comparison
Gam 01 Leo		2.01	K0III	-0.44 ± 0.03	1.59 ± 0.12	2	Giant star, planet host
50671	89707	7.17	G1V	-0.53 ± 0.03	0.84 ± 0.01	3	High-mass brown dwarf
50887	90043	7.38	G5	-0.09 ± 0.02	1.31 ± 0.03	2	Giant star, two planets
51317		9.70	M2	-0.17 ± 0.09	0.41 ± 0.06	5	M dwarf, comparison
51459	90839	4.82	F8V	-0.11 ± 0.01	1.07 ± 0.01	1	Debris disc
52278	92320	8.38	G0	-0.06 ± 0.01	0.98 ± 0.01	3	High-mass brown dwarf
52409	92788	7.31	G5	0.31 ± 0.02	1.11 ± 0.01	4	Two cool planets
52462	92945	7.72	K1V	-0.04 ± 0.03	0.84 ± 0.02	1	Debris disc
53252	94388	5.23	F6V	-0.02 ± 0.04	1.43 ± 0.03	1	Comparison sample
BD-103166		10.01	K3V	0.40 ± 0.05	1.00 ± 0.02	4	Hot planet
53666	95089	7.92	K0 D	0.00 ± 0.02	1.48 ± 0.09	2	Giant star, planet host
53721	95128	5.03	G0V	0.01 ± 0.01	1.03 ± 0.01	1	Cool planet
54195	96167	8.09	G5	0.34 ± 0.03	1.31 ± 0.07	4	Subgiant star, planet host
54532		10.40	M2	-0.10 ± 0.09	0.45 ± 0.05	5	M dwarf, comparison
54745	97334	6.41	G0V	0.10 ± 0.03	1.10 ± 0.01	1	Comparison sample
54906	97658	7.76	K1V	-0.26 ± 0.03	0.78 ± 0.02	1	Low-mass planet
55409	98649	8.00	G3/G5V	-0.06 ± 0.02	0.95 ± 0.02	4	Cool planet
55664	99109	9.10	K0	0.43 ± 0.04	0.98 ± 0.02	4	Cool planet
55848	99492	7.58	K2V	0.45 ± 0.04	$0.48 \pm 0.51^{\ddagger}$	1	Cool planet
56452	100623	5.96	K0V	-0.35 ± 0.02	0.74 ± 0.01	1	Comparison sample
56528		9.80	M1.5	-0.13 ± 0.09	0.47 ± 0.05	5	M dwarf, two planets
56830	101259	6.40	G6/G8V	-0.86 ± 0.01		1	Debris disc, giant?
56997	101501	5.31	G8V	-0.02 ± 0.01	0.96 ± 0.01	1	Comparison sample
57157	101886	10.40	M1	-0.27 ± 0.09	0.43 ± 0.05	5	M dwarf, comparison
57172	101930	8.21	K1V	0.27 ± 0.03	0.93 ± 0.01	4	Cool planet
57370	102195	8.07	K0	0.09 ± 0.02	0.93 ± 0.01	4	Hot planet
57428	102272	8.71	K0	-0.41 ± 0.03	1.05 ± 0.12	2	Giant star, two planets
57443	102365	4.89	G3/G5V	-0.31 ± 0.01	0.83 ± 0.00	1	Low-mass planet
57507	102438	6.48	G5V	-0.29 ± 0.01	0.81 ± 0.00	1	Comparison sample
57548		11.10	M4	-0.25 ± 0.09	0.23 ± 0.10	5	M dwarf, 1 low-mass planet
57820	102956	8.00	A	0.14 ± 0.04	1.56 ± 0.09	2	Giant star, planet host
58237	103720	9.50	K3V	0.07 ± 0.03	0.83 ± 0.02	4	Hot planet
58263	103774	7.13	F5	0.14 ± 0.04	1.34 ± 0.02	4	Hot planet
58451	104067	7.92	K2V	0.10 ± 0.03	0.83 ± 0.02	1	Debris disc and planet
58576	104304	5.54	K0IV	0.30 ± 0.02	1.05 ± 0.02	1	Debris disc

Table A.1. Continued.

HIP/Other	HD	V (mag)	SpType	[Fe/H] (dex)	M_{\star} (M_{\odot})	Ref [†]	Sample/Notes
58952	104985	5.79	G9III	-0.36 ± 0.02	1.22 ± 0.05	2	Giant star, planet host
59285	105639	5.95	K3III	0.09 ± 0.05	1.35 ± 0.08	2	Giant star, comparison sample
59646	106314	6.91	G5	0.10 ± 0.03	1.52 ± 0.03	2	Giant star, comparison sample
59847	106714	4.93	K0III	-0.20 ± 0.03	1.61 ± 0.12	2	Giant star, comparison sample
59856	106760	4.99	K1III	-0.12 ± 0.05	1.85 ± 0.14	2	Giant star, comparison sample
60025	107067	8.69	F8	-0.16 ± 0.03	1.12 ± 0.02	1	Debris disc
60074	107146	7.04	G2V	-0.07 ± 0.02	1.03 ± 0.01	1	Debris disc
60081	107148	8.01	G5	0.26 ± 0.01	1.10 ± 0.01	1	Cool planet
60202	107383	4.72	G8III	-0.31 ± 0.02	2.02 ± 0.11	3	Low-mass brown dwarf
NGC4349-127		10.82	K	-0.18 ± 0.05	$0.64 \pm 0.52^{\ddagger}$	3	Low-mass brown dwarf
60559		11.30	M2.5	-0.33 ± 0.09	0.23 ± 0.10	5	M dwarf, comparison
60585	108103	8.55	G5	0.31 ± 0.04	1.13 ± 0.03	2	Subgiant star, comparison sample
60644	108147	6.99	F8/G0V	0.05 ± 0.01	1.15 ± 0.01	4	Cool planet
61028	108874	8.76	G5	0.26 ± 0.03	1.03 ± 0.02	1	Debris disc and 2 planets
61100	109011	8.08	K2V	-0.18 ± 0.05	0.79 ± 0.02	1	Comparison sample
61595	109749	8.08	G3V	0.21 ± 0.02	1.11 ± 0.02	4	Hot planet
61629		10.70	M3	0.00 ± 0.09	0.43 ± 0.07	5	M dwarf, comparison
61740	110014	4.66	K2III	0.35 ± 0.06	2.94 ± 0.10	2	Giant star, 2 planets
62145	110883	7.01	K3V	0.13 ± 0.04	0.85 ± 0.02	1	Comparison sample
62207	110897	5.95	G0V	-0.60 ± 0.01		1	Debris disc
62523	111395	6.29	G7V	0.11 ± 0.02	1.02 ± 0.01	1	Comparison sample
62534	111232	7.59	G5V	-0.43 ± 0.01	0.77 ± 0.01	4	Cool planet
63033	112164	5.89	G2IV	0.31 ± 0.02	1.49 ± 0.02	1	Comparison sample
63742	113449	7.69	G5V	-0.09 ± 0.04	0.84 ± 0.02	1	Comparison sample
64394	114710	4.23	G0V	0.06 ± 0.02	1.12 ± 0.02	1	Comparison sample
64408	114613	4.85	G3V	0.12 ± 0.01	1.26 ± 0.01	2	Subgiant star, comparison sample
64426	114762	7.30	F9V	-0.74 ± 0.02	0.85 ± 0.00	3	Low-mass brown dwarf
64457	114783	7.56	K0	0.18 ± 0.07	0.87 ± 0.02	4	Two cool planets
64459	114729	6.68	G0V	-0.34 ± 0.01	0.93 ± 0.01	4	Cool planet
64792	115383	5.19	G0V	0.18 ± 0.04	1.21 ± 0.02	1	Cool planet
64797	115404	6.49	K2V	-0.11 ± 0.03	0.80 ± 0.02	1	Comparison sample
64924	115617	4.74	G5V	-0.02 ± 0.01	0.92 ± 0.01	1	Debris disc and 3 low-mass planets
65515	116956	7.29	G9IV-V	0.09 ± 0.04	0.94 ± 0.01	1	Comparison sample
65530	117043	6.50	G6V	0.16 ± 0.03	0.98 ± 0.02	1	Comparison sample
65721	117176	4.97	G5V	-0.11 ± 0.01	1.07 ± 0.01	1	Debris disc and planet
65808	117207	7.26	G8IV/V	0.22 ± 0.02	1.03 ± 0.01	4	Cool planet
65859		9.10	M1	-0.14 ± 0.09	0.51 ± 0.05	5	M dwarf, comparison
66047	117618	7.17	G2V	-0.03 ± 0.01	1.04 ± 0.01	4	Two cool planets
66192	118203	8.05	K0	0.12 ± 0.06	1.25 ± 0.07	4	Subgiant star, planet host
66704	119124	6.31	F7.7V	-0.31 ± 0.05	1.02 ± 0.04	1	Debris disc
66781	119332	7.77	K0IV-V	-0.04 ± 0.03	0.86 ± 0.02	1	Debris disc
67155	119850	8.50	M2	-0.10 ± 0.09	0.47 ± 0.05	5	M dwarf, comparison
67275	120136	4.50	F7V	0.36 ± 0.04	1.41 ± 0.00	4	Hot planet
67422	120476	7.05	K2	0.06 ± 0.05	0.78 ± 0.01	1	Comparison sample
67620	120690	6.43	G5V	0.03 ± 0.03	1.00 ± 0.02	1	Comparison sample
68184	122064	6.49	K3V	0.29 ± 0.04	0.83 ± 0.02	1	Comparison sample
68469	122303	9.70	M1	-0.08 ± 0.09	0.52 ± 0.05	5	M dwarf, low-mass planet
68578	122562	7.69	G5	0.31 ± 0.04	1.12 ± 0.04	3	Low-mass brown dwarf
68593	122652	7.16	F8	0.00 ± 0.02	1.14 ± 0.02	1	Debris disc
68682	122742	6.27	G8V	0.05 ± 0.03	0.99 ± 0.02	1	Comparison sample
68904	123351	7.58	K0	0.03 ± 0.03	1.32 ± 0.06	2	Giant star, comparison sample
69090	122862	6.02	G1V	-0.20 ± 0.01	1.02 ± 0.01	1	Comparison sample
69185	123929	7.28	G8V	-0.29 ± 0.02	1.29 ± 0.05	2	Giant star, comparison sample
69427	124294	4.18	K3III	-0.43 ± 0.04	1.00 ± 0.06	2	Giant star, comparison sample
69612	124679	5.29	K1III	-0.08 ± 0.03	1.61 ± 0.11	2	Giant star, comparison sample
69965	125276	5.87	F7V	-0.65 ± 0.03	0.83 ± 0.02	1	Comparison sample
70027	125560	4.84	K3III	0.27 ± 0.07	1.29 ± 0.20	2	Giant star, comparison sample
70038	125490	6.42	G5	-0.04 ± 0.03	2.04 ± 0.07	2	Giant star, comparison sample
70319	126053	6.25	G1V	-0.28 ± 0.03	0.86 ± 0.02	1	Comparison sample
70616	126647	7.20	K0	0.35 ± 0.06	1.36 ± 0.03	2	Subgiant star, comparison sample

Table A.1. Continued.

HIP/Other	HD	V (mag)	SpType	[Fe/H] (dex)	M_{\star} (M_{\odot})	Ref [†]	Sample/Notes
70695	126525	7.85	G5V	-0.05 ± 0.01	0.95 ± 0.02	4	Cool planet
70857	128642	6.88	G5	-0.03 ± 0.03	0.94 ± 0.02	1	Comparison sample
70890		11.10	M4.5	-0.03 ± 0.09	0.47 ± 0.06	5	M dwarf, 1 low-mass planet
71181	128165	7.24	K3V	-0.04 ± 0.05	0.76 ± 0.02	1	Debris disc
71395	128311	7.48	K0	0.09 ± 0.03	0.83 ± 0.01	4	Debris discs and 2 planets
71681	128621	1.35	K1V	0.26 ± 0.03	0.94 ± 0.02	1	Low-mass planet
71683	128620	-0.01	G2V	0.23 ± 0.02	1.10 ± 0.01	1	Comparison sample
71743	128987	7.24	G6V	0.14 ± 0.04	0.98 ± 0.01	1	Comparison sample
72339	130322	8.04	K0III	0.06 ± 0.01	0.94 ± 0.02	4	Debris disc and planet
72567	130948	5.86	G2V	-0.07 ± 0.02	1.05 ± 0.02	1	Comparison sample
72848	131511	6.00	K2V	0.14 ± 0.03	0.93 ± 0.01	1	Debris disc
72944		10.20	M2	-0.02 ± 0.09	0.50 ± 0.05	5	M dwarf, comparison
73100	132254	5.63	F7V	0.05 ± 0.03	1.24 ± 0.02	1	Debris disc
73128	132032	8.11	G5	0.09 ± 0.01	1.10 ± 0.01	3	High-mass brown dwarf
73408	131664	8.13	G3V	0.30 ± 0.01	1.15 ± 0.01	3	Low-mass brown dwarf
73869	134319	8.40	G5	-0.25 ± 0.04	0.91 ± 0.03	1	Debris disc
74033	134113	8.26	F9V	-0.92 ± 0.02	0.85 ± 0.02	3	High-mass brown dwarf
74500	134987	6.47	G5V	0.27 ± 0.02	1.10 ± 0.01	4	Two cool planets
74702	135599	6.92	K0	-0.07 ± 0.02	0.86 ± 0.01	1	Debris disc
74793	136726	5.02	K4III	0.00 ± 0.06	1.69 ± 0.18	2	Giant star, planet host
74948	136118	6.93	F8	-0.17 ± 0.06	1.12 ± 0.04	3	Low-mass brown dwarf
74961	136418	7.88	G5	-0.11 ± 0.02	1.27 ± 0.05	2	Giant star, planet host
74975	136202	5.04	F8III-IV	-0.04 ± 0.02	1.32 ± 0.05	1	Debris disc
74995		10.60	M3	-0.20 ± 0.09	0.29 ± 0.09	5	M dwarf, 3 low-mass planets
75458	137759	3.29	K2III	0.27 ± 0.07	1.78 ± 0.23	3	Giant, debris discs and low-mass BD
75535	137510	6.26	G0V	0.25 ± 0.03	1.39 ± 0.03	3	Low-mass brown dwarf
76074		9.30	M3	0.00 ± 0.09	0.46 ± 0.06	5	M dwarf, comparison
76311	139357	5.98	K4III	0.34 ± 0.05	2.16 ± 0.18	2	Giant star, planet host
76375	139323	7.65	K3V	0.37 ± 0.03	0.90 ± 0.02	1	Debris disc
76635	139590	7.50	G0V	0.06 ± 0.01	1.19 ± 0.02	1	Debris disc
77052	140538	5.86	G5V	0.12 ± 0.02	1.05 ± 0.01	1	Comparison sample
77152	140913	8.06	G0V	-0.08 ± 0.07	1.02 ± 0.04	3	High-mass brown dwarf
77372	141128	7.00	F5	0.10 ± 0.03	1.37 ± 0.02	1	Comparison sample
77408	141272	7.44	G8V	-0.04 ± 0.03	0.88 ± 0.02	1	Comparison sample
77517	330075	9.36	G5	0.18 ± 0.04	0.86 ± 0.02	4	Hot planet
77655	142091	4.79	K1IV	0.09 ± 0.02	1.46 ± 0.03	2	Giant star, planet host
77760	142373	4.60	F9V	-0.62 ± 0.02	0.91 ± 0.00	1	Comparison sample
77801	142267	6.07	G0IV	-0.44 ± 0.01	0.82 ± 0.01	1	Comparison sample
77838	143105	6.76	F5	0.03 ± 0.08	1.33 ± 0.04	4	Hot planet
78072	142860	3.85	F6V	-0.29 ± 0.04	1.10 ± 0.03	1	Comparison sample
78169	142415	7.33	G1V	0.08 ± 0.02	1.09 ± 0.01	4	Cool planet
78459	143761	5.39	G2V	-0.30 ± 0.02	0.91 ± 0.00	1	Two planets
78521	143361	9.20	G6V	0.32 ± 0.04	1.05 ± 0.02	4	Cool planet
78775	144579	6.66	G8V	-0.67 ± 0.03		1	Comparison sample
79219	145457	6.57	K0	-0.20 ± 0.03	1.24 ± 0.24	2	Giant star, planet host
79248	145675	6.61	K0V	0.50 ± 0.06	0.98 ± 0.02	1	Cool planet
79492	145958	6.68	G8V	0.14 ± 0.03	0.95 ± 0.02	1	Debris disc
79672	146233	5.49	G1V	0.07 ± 0.02	1.06 ± 0.02	1	Comparison sample
80018		10.60	M3	-0.10 ± 0.09	0.37 ± 0.08	5	M dwarf, comparison
80337	147513	5.37	G3/G5V	0.03 ± 0.01	1.07 ± 0.01	4	Cool planet
80680	148156	7.69	G1V	0.24 ± 0.04	1.24 ± 0.02	4	Cool planet
80687	148427	6.89	K0IV	0.06 ± 0.03	1.40 ± 0.03	2	Giant star, planet host
80725	148653	6.98	K2V	-0.33 ± 0.04	0.78 ± 0.00	1	Comparison sample
80816	148856	2.78	G8III	-0.10 ± 0.03	2.89 ± 0.07	2	Giant star, comparison sample
80824		10.10	M3.5	-0.05 ± 0.09	0.25 ± 0.12	5	M dwarf, 3 low-mass planets
80838	149026	8.15	G0 IV	0.49 ± 0.04	1.36 ± 0.02	2	Hot planet
80902	150706	7.01	G0	-0.09 ± 0.02	1.01 ± 0.02	1	Debris disc and planet
81022	149143	7.89	G0	0.24 ± 0.02	1.20 ± 0.03	4	Hot planet
81300	149661	5.77	K2V	0.09 ± 0.03	0.91 ± 0.01	1	Comparison sample
81800	151044	6.48	F8V	-0.03 ± 0.01	1.10 ± 0.01	1	Debris disc

Table A.1. Continued.

HIP/Other	HD	V (mag)	SpType	[Fe/H] (dex)	M_{\star} (M_{\odot})	Ref [†]	Sample/Notes
81819	150474	7.16	G8V	-0.02 ± 0.01	1.09 ± 0.03	2	Subgiant star, comparison sample
82588	152391	6.65	G8V	-0.01 ± 0.03	0.94 ± 0.02	1	Comparison sample
82817	152751	11.80	M2.5	0.08 ± 0.10	0.45 ± 0.08	5	M dwarf, comparison
82860	153597	4.88	F6V	-0.07 ± 0.03	1.19 ± 0.02	1	Comparison sample
83389	154345	6.76	G8V	-0.09 ± 0.02	0.90 ± 0.02	1	Two cool planets
83983	154672	8.21	G3IV	0.24 ± 0.03	1.10 ± 0.03	4	Cool planet
GJ667C		10.20	M1	$-0.55 \pm 0.10^{\ddagger}$	$0.33 \pm 0.02^{\ddagger}$	5	M dwarf, 5/6? low-mass planets
84856	156846	6.50	G1V	0.13 ± 0.01	1.36 ± 0.04	3	Low-mass brown dwarf
84862	157214	5.38	G0V	-0.39 ± 0.02		1	Comparison sample
84975	157261	6.67	G5	-0.17 ± 0.02	1.42 ± 0.05	2	Giant star, comparison sample
85235	158633	6.44	K0V	-0.44 ± 0.02	0.74 ± 0.01	1	Debris disc
85523		9.40	M2.5	-0.20 ± 0.09	0.36 ± 0.07	5	M dwarf, 1 low-mass planet
85665		9.30	M0	-0.09 ± 0.09	0.58 ± 0.06	5	M dwarf, comparison
86036	160269	5.23	G0V	0.03 ± 0.02	1.08 ± 0.02	1	Comparison sample
86057		10.20	M2	-0.12 ± 0.09	0.45 ± 0.05	5	M dwarf, comparison
86214		11.00	M4	0.02 ± 0.09	0.35 ± 0.10	5	M dwarf, comparison
86287		9.60	M1	-0.26 ± 0.09	0.44 ± 0.05	5	M dwarf, comparison
86394	160508	8.11	F8V	-0.16 ± 0.02	1.14 ± 0.04	3	High-mass brown dwarf
86796	160691	5.12	G5V	0.25 ± 0.02	1.13 ± 0.02	1	Three giant planets, 1 low-mass planet
86990		10.80	M3	-0.27 ± 0.09	0.23 ± 0.10	5	M dwarf, comparison
87330	162020	9.10	K2V	0.00 ± 0.04	0.76 ± 0.02	3	Low-mass
TrES-4		11.59	F	0.40 ± 0.05	1.48 ± 0.03	2	Hot planet
88048	163917	3.33	G9III	0.15 ± 0.04	3.04 ± 0.05	2	Giant, two low-mass brown dwarfs
88414	164604	9.62	K2	0.28 ± 0.06	0.82 ± 0.02	4	Cool planet
88574	165222	9.40	M1	-0.19 ± 0.09	0.46 ± 0.05	5	M dwarf, comparison
88601	165341	4.03	K0V	0.07 ± 0.02	0.90 ± 0.02	1	Comparison sample
88745	165908	5.05	F7V	-0.60 ± 0.01	0.85 ± 0.00	1	Debris disc
88765	165760	4.64	G8III-IV	-0.01 ± 0.03	2.68 ± 0.07	2	Giant star, comparison sample
88836	166229	5.49	K2III	0.21 ± 0.06	1.52 ± 0.10	2	Giant star, comparison sample
88972	166620	6.38	K2V	-0.14 ± 0.03	0.78 ± 0.02	1	Comparison sample
89042	165499	5.47	G0V	-0.13 ± 0.01	0.99 ± 0.01	1	Comparison sample
89047	167042	5.97	K1III	0.03 ± 0.02	1.53 ± 0.02	2	Giant star, planet host
89620	167665	6.36	F8V	-0.21 ± 0.01	1.03 ± 0.01	3	High-mass brown dwarf
89826	168775	4.33	K2III	0.13 ± 0.05	2.62 ± 0.18	2	Giant star, comparison sample
89844	168443	6.92	G5	0.01 ± 0.01	1.00 ± 0.01	3	Low-mass brown dwarf and planet
89918	168656	4.85	G8III	-0.09 ± 0.02	2.45 ± 0.07	2	Giant star, comparison sample
89962	168723	3.23	K0III-IV	-0.19 ± 0.02	1.45 ± 0.04	2	Giant star, comparison sample
90004	168746	7.95	G5	-0.07 ± 0.01	0.90 ± 0.01	4	Hot planet
90344	170693	4.83	K1.5III	-0.34 ± 0.03	1.37 ± 0.21	2	Giant star, planet host
90485	169830	5.90	F8V	0.03 ± 0.01	1.34 ± 0.04	1	Two cool planets
90593	170469	8.21	G5	0.28 ± 0.02	1.14 ± 0.03	4	Cool planet
91258		8.65	G5	0.23 ± 0.03	1.00 ± 0.02	4	Hot planet
91438	172051	5.85	G5V	-0.25 ± 0.01	0.84 ± 0.01	1	Comparison sample
91852	173416	6.06	G8	-0.12 ± 0.04	1.83 ± 0.24	2	Giant star, planet host
92043	173667	4.19	F6V	-0.21 ± 0.05	1.34 ± 0.04	1	Debris disc
92403		10.50	M3.5	-0.06 ± 0.10	0.46 ± 0.06	5	M dwarf, comparison
92418	174457	7.52	F8	-0.26 ± 0.02	0.96 ± 0.02	3	High-mass brown dwarf
92895	175541	8.03	G8IV	-0.07 ± 0.04	1.42 ± 0.10	2	Giant star, planet host
92968	175679	6.14	G8III	-0.01 ± 0.05	2.53 ± 0.12	3	Low-mass brown dwarf
93017	176051	5.20	G0V	-0.07 ± 0.05	1.02 ± 0.03	1	Cool planet
93746	177830	7.18	K0IV	0.47 ± 0.06	1.35 ± 0.04	2	Subgiant star, two planets
93858	177565	6.15	G8V	0.10 ± 0.01	0.98 ± 0.01	1	Comparison sample
94050	177996	7.89	K1V	-0.04 ± 0.05	0.86 ± 0.02	1	Debris disc
94256	179079	7.95	G5IV	0.33 ± 0.04	1.20 ± 0.04	2	Subgiant star, planet host
94346	180161	7.04	G8V	0.16 ± 0.03	0.96 ± 0.01	1	Comparison sample
94576	180314	6.61	K0	0.24 ± 0.07	2.13 ± 0.13	3	Giant, Low-mass brown dwarf and planet
94645	179949	6.25	F8V	0.12 ± 0.02	1.20 ± 0.01	4	Hot planet
94761	180617	9.10	M3	0.02 ± 0.09	0.49 ± 0.06	5	M dwarf, comparison
94858	180134	6.36	F7V	-0.30 ± 0.01	1.15 ± 0.01	1	Debris disc
94951	180902	7.78	K0III/IV	0.01 ± 0.03	1.49 ± 0.07	2	Giant star, planet host

Table A.1. Continued.

HIP/Other	HD	V (mag)	SpType	[Fe/H] (dex)	M_{\star} (M_{\odot})	Ref [†]	Sample/Notes
95124	181342	7.55	K0III	0.20 ± 0.03	1.71 ± 0.07	2	Giant star, planet host
95149	181321	6.48	G1/G2V	-0.11 ± 0.03	0.99 ± 0.02	1	Comparison sample
95319	182488	6.37	G8V	0.20 ± 0.02	0.99 ± 0.01	1	High-mass brown dwarf
95740	183263	7.86	G2IV	0.47 ± 0.04	1.24 ± 0.02	2	Two cool planets
HAT-P-7		10.50		0.23 ± 0.03	1.49 ± 0.14	2	Subgiant star, planet host + BD
95822	183492	5.57	K0III	0.07 ± 0.03	1.92 ± 0.14	2	Giant star, comparison sample
95926	183756	6.91	K0	-0.06 ± 0.02	1.33 ± 0.04	2	Giant star, comparison sample
96016	184010	5.89	K0III-IV	-0.13 ± 0.02	1.57 ± 0.04	2	Giant star, comparison sample
96100	185144	4.67	K0V	-0.18 ± 0.02	0.83 ± 0.02	1	Comparison sample
KOI415			G0IV	0.15 ± 0.07	$1.04 \pm 0.12^{\ddagger}$	3	High-mass brown dwarf
96229	184406	4.45	K3III	0.16 ± 0.06	1.14 ± 0.08	2	Giant star, comparison sample
96441	185395	4.49	F4V	-0.02 ± 0.02	1.37 ± 0.02	1	Comparison sample
96507	185269	6.67	G0IV	0.14 ± 0.04	1.35 ± 0.05	2	Subgiant star, planet host
96901	186427	6.25	G5V	0.08 ± 0.02	1.02 ± 0.01	1	Cool planet
97336	187123	7.83	G5	0.13 ± 0.02	1.07 ± 0.01	4	Two hot planets
97546	187085	7.22	G0V	0.03 ± 0.01	1.12 ± 0.01	4	Debris disc and planet
97675	187691	5.12	F8V	0.06 ± 0.01	1.20 ± 0.02	1	Comparison sample
97938	188310	4.72	G9III	-0.15 ± 0.04	1.43 ± 0.34	2	Giant star, planet host
98036	188512	3.71	G8IV	-0.19 ± 0.01	1.32 ± 0.01	2	Subgiant star, comparison sample
98138	188993	6.80	G2III	0.04 ± 0.03	1.62 ± 0.06	2	Subgiant star, comparison sample
98210	188844	6.56	G5	-0.17 ± 0.03	1.31 ± 0.07	2	Giant star, comparison sample
98314	189186	6.77	K0	-0.36 ± 0.02	1.30 ± 0.05	2	Giant star, comparison sample
98714	190228	7.30	G5IV	-0.33 ± 0.02	1.12 ± 0.04	3	High-mass brown dwarf
98767	190360	5.71	G6 IV	0.23 ± 0.02	1.02 ± 0.01	2	One giant and one low-mass planet
98819	190406	5.80	G1V	-0.01 ± 0.02	1.05 ± 0.02	3	High-mass brown dwarf
98845	190571	7.47	G8V	-0.25 ± 0.04	1.27 ± 0.06	2	Giant star, comparison sample
98920	190608	5.09	K2III	0.09 ± 0.04	1.60 ± 0.08	2	Giant star, comparison sample
98959	189567	6.07	G2V	-0.28 ± 0.01	0.85 ± 0.00	1	Low-mass planet
99115	190647	7.78	G5V	0.23 ± 0.02	1.08 ± 0.02	4	Cool planet
99171	191067	5.97	K1IV	-0.04 ± 0.03	1.07 ± 0.05	2	Giant star, comparison sample
99240	190248	3.55	G5IV-V	0.34 ± 0.02	1.06 ± 0.01	1	Comparison sample
99316	191499	7.56	K0	-0.13 ± 0.03	0.84 ± 0.02	1	Debris disc
99461	191408	5.32	K2V	-0.49 ± 0.02	0.69 ± 0.00	1	Comparison sample
99661	191760	8.26	G3IV/V	0.24 ± 0.01	1.23 ± 0.04	3	Low-mass brown dwarf
99711	192263	7.79	K0	0.04 ± 0.02	0.84 ± 0.01	4	Debris disc and planet
99825	192310	5.73	K3V	0.08 ± 0.03	0.86 ± 0.02	1	Two low-mass planet
99841	192787	5.70	K0III	-0.11 ± 0.02	2.16 ± 0.09	2	Giant star, comparison sample
99894	192699	6.44	G8IV	-0.19 ± 0.03	1.48 ± 0.05	2	Giant star, planet host
99913	192836	6.11	K1III	0.07 ± 0.03	1.87 ± 0.05	2	Giant star, comparison sample
100022	193343	7.70	K2	0.18 ± 0.04	1.42 ± 0.05	2	Giant star, comparison sample
100503	194110	7.21	K0	-0.22 ± 0.01	1.39 ± 0.03	2	Giant star, comparison sample
100541	194013	5.30	G8III-IV	-0.06 ± 0.03	1.95 ± 0.10	2	Giant star, comparison sample
100587	194317	4.43	K3III	0.01 ± 0.06	1.31 ± 0.18	2	Giant star, comparison sample
100970	195019	6.91	G3 IV-V	0.09 ± 0.03	1.07 ± 0.02	2	Subgiant star, planet host
101806	196050	7.50	G3V	0.19 ± 0.01	1.14 ± 0.03	4	Cool planet
101848	196645	7.80	K0	-0.17 ± 0.02	1.28 ± 0.05	2	Giant star, comparison sample
101936	196758	5.15	K1III	0.07 ± 0.05	1.83 ± 0.13	2	Giant star, comparison sample
101983	196378	5.11	F8V	-0.44 ± 0.01	1.07 ± 0.00	1	Comparison sample
101997	196761	6.36	G8/K0V	-0.25 ± 0.02	0.81 ± 0.02	1	Comparison sample
102125	196067	6.51	G1V	0.13 ± 0.02	1.27 ± 0.09	4	Cool planet
102409	197481	8.80	M0.5			5	M dwarf, comparison
102531	197963	5.15	A2Ia	0.08 ± 0.02	1.62 ± 0.03	2	Subgiant star, comparison sample
102532	197964	4.27	K1IV	0.13 ± 0.03	1.94 ± 0.05	2	Giant star, comparison sample
103004	198809	4.56	G8III	-0.05 ± 0.02	2.40 ± 0.05	2	Giant star, comparison sample
103389	199260	5.70	F7V	-0.15 ± 0.03	1.12 ± 0.02	1	Debris disc
103519	199870	5.55	G8III	0.12 ± 0.03	2.33 ± 0.05	2	Giant star, comparison sample
103527	199665	5.52	G6III	0.07 ± 0.04	2.28 ± 0.04	2	Giant star, planet host
104202	200964	6.64	K0	-0.11 ± 0.03	1.53 ± 0.05	2	Giant star, two planets
104239	200968	7.12	K1V	0.05 ± 0.05	0.87 ± 0.02	1	Debris disc
104903	202206	8.08	G6V	0.29 ± 0.01	1.10 ± 0.01	3	Debris discs and low-mass BD

Table A.1. Continued.

HIP/Other	HD	V (mag)	SpType	[Fe/H] (dex)	M_{\star} (M_{\odot})	Ref [†]	Sample/Notes
105312	202940	6.56	G5V	-0.31 ± 0.02	0.81 ± 0.00	1	Comparison sample
105388	202917	8.65	G5V	-0.33 ± 0.05	0.83 ± 0.03	1	Debris disc
105390	203358	6.45	G8IV	-0.23 ± 0.02	1.40 ± 0.04	2	Giant star, comparison sample
105411	203344	5.58	K1III	-0.10 ± 0.03	1.77 ± 0.15	2	Giant star, comparison sample
105502	203504	4.08	K1III	0.00 ± 0.03	1.47 ± 0.11	2	Giant star, comparison sample
105858	203608	4.21	F6V	-0.76 ± 0.02		1	Comparison sample
106081	204642	6.75	K2III	0.11 ± 0.04	1.41 ± 0.09	2	Giant star, comparison sample
106093	204771	5.22	K0III	0.06 ± 0.03	2.02 ± 0.07	2	Giant star, comparison sample
106440	204961	8.70	M2	-0.16 ± 0.09	0.44 ± 0.05	5	M dwarf, 2 planets
106696	205390	7.14	K2V	-0.17 ± 0.02	0.80 ± 0.01	1	Comparison sample
107022	205536	7.07	G8V	-0.03 ± 0.01	0.88 ± 0.01	1	Debris disc
107251	206610	8.34	K0	0.22 ± 0.06	1.74 ± 0.21	2	Giant star, planet host
107350	206860	5.96	G0V	-0.20 ± 0.03	0.98 ± 0.02	1	Debris disc and brown dwarf
107649	207129	5.57	G2V	-0.09 ± 0.02	0.99 ± 0.01	1	Debris disc
107985	207832	8.78	G5V	0.17 ± 0.01	1.08 ± 0.01	4	Two cool planets
108028	208038	8.18	K0	-0.08 ± 0.04	0.80 ± 0.02	1	Debris disc
108761	209262	8.00	G5	0.06 ± 0.01	1.00 ± 0.01	3	Low-mass brow dwarf
108782	209290	9.20	M0	-0.09 ± 0.09	0.59 ± 0.06	5	M dwarf, comparison
109378	210277	6.54	G0	0.19 ± 0.02	0.96 ± 0.01	4	Debris disc and planet
109388		10.40	M3.5	0.12 ± 0.09	0.48 ± 0.07	5	M dwarf, 2 planets
109422	210302	4.94	F6V	-0.01 ± 0.04	1.24 ± 0.02	1	Comparison sample
109577	210702	5.93	K1III	0.02 ± 0.02	1.63 ± 0.03	2	Giant star, planet host
109822	211038	6.55	K0/K1V	-0.30 ± 0.01	0.93 ± 0.00	2	Subgiant star, comparison sample
109821	210918	6.23	G5V	-0.11 ± 0.01	0.92 ± 0.01	1	Comparison sample
110109	211415	5.36	G1V	-0.30 ± 0.02	0.87 ± 0.00	1	Comparison sample
110538	212496	4.42	G9III	-0.30 ± 0.02	1.39 ± 0.11	2	Giant star, comparison sample
110813	212771	7.60	G8IV	-0.17 ± 0.02	1.49 ± 0.10	2	Giant star, planet host
110852	212301	7.76	F8V	0.18 ± 0.02	1.25 ± 0.02	4	Hot planet
111143	213240	6.81	G4IV	0.05 ± 0.01	1.11 ± 0.01	4	Cool planet
111944	214868	4.50	K3III	-0.19 ± 0.05	1.66 ± 0.16	2	Giant star, comparison sample
112041	215030	5.93	G9III	-0.42 ± 0.02	1.21 ± 0.06	2	Giant star, comparison sample
112067	214995	5.92	K0III	-0.01 ± 0.05	1.49 ± 0.09	2	Giant star, comparison sample
112158	215182	2.93	G2II-III	-0.21 ± 0.03	3.30 ± 0.09	2	Giant star, comparison sample
112190	215152	8.11	K0	0.05 ± 0.06	0.80 ± 0.02	1	Debris disc and 4 low-mass planets
112242	215373	5.11	K0III	0.10 ± 0.03	2.59 ± 0.04	2	Giant star, comparison sample
113020		10.20	M4	0.16 ± 0.09	0.35 ± 0.11	5	M dwarf, 4 planets
113044	216435	6.03	G3IV	0.18 ± 0.02	1.29 ± 0.04	4	Debris disc and planet
113137	216437	6.04	G4IV-V	0.18 ± 0.01	1.13 ± 0.03	4	Cool planet
113229		10.40	M3	-0.11 ± 0.09	0.34 ± 0.09	5	M dwarf, comparison
113238	216770	8.11	K0V	0.34 ± 0.03	1.01 ± 0.02	4	Cool planet
113296	216899	8.70	M1.5	-0.01 ± 0.09	0.57 ± 0.05	5	M dwarf, comparison
113357	217014	5.45	G5V	0.22 ± 0.04	1.11 ± 0.02	4	Hot planet
113421	217107	6.17	G8IV	0.37 ± 0.02	1.07 ± 0.01	4	Two planets
113698		9.77	K2	-0.16 ± 0.03	0.75 ± 0.02	3	High-mass brown dwarf
113834	217786	7.78	F9V	-0.19 ± 0.01	0.96 ± 0.01	3	Low-mass brown dwarf
114046	217987	7.30	M1	-0.18 ± 0.09	0.49 ± 0.05	5	M dwarf, comparison
114236	218340	8.44	G3V	0.07 ± 0.01	1.09 ± 0.02	1	Debris disc
	240210	8.33	K3III	-0.11 ± 0.06	1.10 ± 0.11	2	Giant star, planet host
114622	219134	5.57	K3V	0.16 ± 0.04	0.81 ± 0.02	1	Five low-mass planets, one cool giant
114699	219077	6.12	G5IV	-0.18 ± 0.01	1.03 ± 0.01	3	Subgiant star, low-mass brown dwarf
114855	219449	4.21	K0 III	0.00 ± 0.04	1.19 ± 0.12	2	Giant star, planet host
114948	219482	5.64	F7V	-0.04 ± 0.02	1.16 ± 0.02	1	Debris disc
115100	219828	8.04	G0IV	0.12 ± 0.02	1.13 ± 0.04	2	Subgiant star, two planets
115331	220182	7.36	K1V	0.03 ± 0.03	0.92 ± 0.01	1	Comparison sample
115662	220689	7.74	G3V	-0.07 ± 0.01	0.99 ± 0.01	4	Cool planet
115696	220807	6.81	G5	-0.40 ± 0.02	1.02 ± 0.04	2	Giant star, comparison sample
115830	220954	4.27	K1III	0.08 ± 0.04	1.83 ± 0.05	2	Giant star, comparison sample
115919	221115	4.54	G8III	0.05 ± 0.03	2.39 ± 0.06	2	Giant star, comparison sample
116076	221345	5.22	K0III	-0.26 ± 0.02	1.08 ± 0.09	2	Giant star, planet host
116250	221420	5.82	G2V	0.26 ± 0.01	1.34 ± 0.04	2	Subgiant star, comparison sample

Table A.1. Continued.

HIP/Other	HD	V (mag)	SpType	[Fe/H] (dex)	M _★ (M _☉)	Ref [†]	Sample/Notes
116584	222107	3.81	G8III-IV	-0.42 ± 0.04	1.12 ± 0.08	2	Giant star, comparison sample
116613	222143	6.58	G5	0.18 ± 0.02	1.12 ± 0.00	1	Comparison sample
116745	222237	7.09	K3V	-0.26 ± 0.03	0.70 ± 0.01	1	Comparison sample
116771	222368	4.13	F7V	-0.09 ± 0.02	1.19 ± 0.03	1	Comparison sample
116823	222455	7.40	K3III	0.16 ± 0.06	1.09 ± 0.06	2	Giant star, comparison sample
116906	222582	7.68	G5	-0.02 ± 0.01	0.98 ± 0.01	1	Cool planet
117375	223252	5.49	G8III	-0.05 ± 0.03	2.32 ± 0.09	2	Giant star, comparison sample
117411	223301	7.60	K1III	0.17 ± 0.04	1.20 ± 0.08	2	Giant star, comparison sample
117473		9.00	M1.5	-0.27 ± 0.09	0.39 ± 0.06	5	M dwarf, comparison
117541	223524	5.93	K0IV	0.10 ± 0.05	1.30 ± 0.27	2	Giant star, comparison sample
117828	223889	10.00	M2.5	0.07 ± 0.09	0.52 ± 0.05	5	M dwarf, comparison
118319	224693	8.23	G2IV	0.21 ± 0.02	1.34 ± 0.06	2	Subgiant star, planet host

Notes. [†] Reference for metallicity and stellar mass: (1) Maldonado et al. (2015b); (2) Maldonado & Villaver (2016); (3) Maldonado & Villaver (2017); (4) Maldonado et al. (2018); (5) Maldonado et al. (2015a); [‡] Value from the NASA exoplanet archive. Specifically from the summary of stellar information table for all stars, but KOI 415 for which we took the value from the KOI stellar properites table; ^{a)} Lovis & Mayor (2007); ^{b)} Bouchy et al. (2016); ^{c)} Niedzielski et al. (2009). Mass uncertainties listed as “0.00” should be understood as lower than 0.01 solar masses.